

SUMMARY OF CHANGES

Firstly, we would like to express our thankfulness and appreciation to the reviewers for their useful comments to improve the paper. We have addressed all the comments as explained below.

GENERAL COMMENT: Major changes in the new version of the article

Considering the useful comments of the Referees we proceed to some major changes in the article in order to provide full explanations of the purpose of our experiment and avoid confusion with future works (particularly about the longwave balance). The view factors are based on the equations of sky view factors in Masson, 2000. Those related to the high vegetation are defined on all the directions. In this way, the interactions between all the facets of the canyon, the sky and trees are allowed in Eq. A6, A7, A8. $\Psi(wt)$ is now expressed for one wall. Specific coefficients are applied, in the shortwave scheme only, to constrain the reflections from the high vegetation toward sky and top part of walls. It ensure the compatibility with the calculations of the longwave exchanges, for which the same view factors but no coefficients are involved. The statistics are based on the Mean Absolute Error instead of the Root Mean Square Error, according to the suggestion of the Referee 2 and the Willmott and Matsuura works (2005). The section about the sensibility of TEB model to the vegetation layouts have been removed in absence of clear and systematic behaviors in the simulations. We also permuted the figures 8 and 9 (after removing the former figures 8, 9, 10) and changed the figure 9 about the canyon albedos from a comparison SOLENE vs TEB to a comparison TEB reference vs TEB with a tree canopy layer. The physic assumptions (e.g., the nature of radiation, specular or isotropic, during the multiple reflections) are too different to allow an accurate comparison of absorption by canyon surfaces or canyon albedo. All the figures and text have been adapted.

We payed attention to express better the two major objectives of this work:

- (1) technical objective of evaluating the geometrical assumptions related to the high vegetation by the confrontation with a model with explicit tree crowns where the radiative budget is solved at high resolution (through numerical meshed mock-ups);
- (2) scientific objective for further studies of simulating different vegetation layouts, potentially including urban trees, to provide information about impacts of greening on microclimate, thermal comfort, energy demand by buildings and needs of water to maintain the vegetation at the city-scale.

REFEREE 1 :

PART 1 : Points for Correction and Clarification

1. “ At a number of points you refer to keeping computing times acceptable (e.g. Page 1, Line 7; Page 6, Line 21). It is unclear what is an acceptable computing time is in this context. Do you mean relative to a complex model? How is the representation of this process going to significantly add to computing time? Surely representing the process correctly is more important in the first instance, and computing time shouldn't determine a limit on how we approach a problem from a modelling perspective as computational optimisation and simplification can be applied later. ”

The TEB model (integrated in the SURFEX land-surface modeling system) has been initially developed for mesoscale modeling, with the objective of including the cities in meteorological models and of being able to simulate the urban heat island. Such applications at city scale entail some constraints about the level of accuracy in the description of urban environment. The model does not pretend to explicitly describe the exact arrangement of streets and buildings, but adopts a simplified approach of mean urban canyons which enables to distinguish the main urban typologies. Even if we are working to improve the TEB model by including new physical processes that seem important to us especially for evaluating adaptation and mitigation strategies, we are committed to maintain a certain level of simplicity. Besides the numerical aspects and time computing, we think that uncertainties associated with the prescription of input data (maps of morphological parameters, materials properties, or vegetation characteristics) significantly limit the potential gain of a very complex modeling.

Note that in case of very fine-scale studies, suitable models already exist, e.g. the CFD models, but they are run over much smallest areas.

See page 6 at lines 21-26 the revisions in the paper.

2. “ Page3 Lines 27-31. Since the conference paper of Young et al. (2015) there have been a number of developments relating to the Trees in Urban Areas model (TURban).

The tree representation is not currently implemented within MORUSES (Met Office Reading Urban Surface Exchange Scheme). Instead the scheme has been developed and is currently been tested within the Single Column Reading Urban Model (SCRUM) as described in Harman and Belcher (2006) and Porson et al. (2009).

The view factors for both fully visible and partially occluded facets are calculated analytically based on Hottel’s crossed string construction (Hottel 1954). A paper is about to be submitted on this method to Boundary-Layer Meteorology but unfortunately to have gone through the review process in time for this papers publication (Young et al, 2016). These sentences need amending in light of this new information. ”

We apologize for our confusing description on TURban developments. We noted the Referee's information and consequently amended the text.

See page 3 at lines 28-32 the revisions in the paper.

3. “ Section 3.2. You talk about improvements of the radiation budget but only mention the longwave radiation budget on Page 6 Line 3. How is this to be modelled for the high vegetation? Although the paper is focused on shortwave radiation it would add to the paper if you described briefly how longwave radiation is treated. ”

Here, we made the choice to focus on solar radiation budget for two main reasons.

The comparison to the SOLENE model is not suitable for infrared radiation budget, because the two models deal differently with the resolution of surface turbulent exchanges and the calculation of surface temperatures of urban facets. The comparison SOLENE vs TEB for the calculation of infrared radiation fluxes becomes consequently tricky, since these fluxes are strongly dependent on surface emissions.

The validation of our shortwave radiation scheme contributes to verify our future longwave radiation scheme because the same view factors are used for the calculations of multiple reflections in shortwave radiation but also infrared radiation exchanges.

Specific coefficients are now applied, in the shortwave scheme only, to constrain the reflections

from the high vegetation toward sky and top part of walls. It ensure the compatibility with the calculations of the longwave exchanges, for which the same view factors but no coefficients are involved. In nature, the solar radiation is mainly redirected upwards by the receiving face of sunlit leaves in the top of crown during the first reflection. We suggest here to neglect the small amount of shortwave radiation which the tree stratum is supposed to reflect to the low part of the canyon during multiple reflections in favor of representing realistically the upward first reflection of solar radiation, which is by far the most energetic reflection. On the contrary, emission of longwave radiation by the vegetation is intrinsically isotropic and can reach all the viewed canyon facets. In this case, all the leaves of the crown, statistically associated to all orientations, participate to the emission.

We added further explanations in the paper page 6, at lines 12-17 and page 10-11, at lines 26-28 and 1-5.

4. “ Page 6, Lines 24 – 30. The hypothesis about street trees and why they are confined within the canyon is not particularly compelling without explicit examples of such rules on tree management and location. Is this specific to France? Surely the justification is more to do with the model assumptions of the canyon and roof being treated separately in the modelling of the surface energy balance in that the canyon and roof are assumed to be independent of each other? Either that or are you just considering the effects of trees that are not taller than the buildings, as to consider these is not possible within the current TEB configuration? ”

Choices on model developments are firstly driven by observations. We refer to the typical positions of trees in urban environment. Depending on the urban form, we observe different vegetation layouts in the townscape. Large avenues of six or height-storey buildings are generally tree-filled with a double row of trees (e.g., *Aesculus hippocastanum*, *Platanus x acerifolia*) which the mature height is near the same of the buildings height, around 20 m. The top of trees is commonly cut in order to provide neat and homogeneous sky line and facilitate the long-term management. Along the second or third order streets axes, smaller trees are planted such as *Tilia x euchlora* or *Acer platanoides* 'Globosum'. At the center of urban groups, squares are greened with grass and trees. In addition to the road, the places are surrounded by wide walkways and recreational areas equipped by benches; so the distance from trees to buildings is significant. Some single specimens can be found in crossroads of boulevards and second order streets or at roundabouts. Each planting in the public area of cities is submitted to compliance with the local tree management rules. These documents are precisely specifying species chosen in adequacy with the aspect ratio of the street, function and aesthetic of the site. They ensure a satisfactory juxtaposition of trees with urban structures for the dwellers (by avoiding excessive shade of trees on facades or disruption of underground services by roots) but also prevent damages of roots by potential new soil removing. It is stated as fundamental urban design principle that streets with 1:1.4 aspect ratio are unsuitable for tree planting. Typically, trunks are planted at least at 3 to 5 meters from walls or balconies. The minimum distance between crowns and walls or balconies is 1.5 meters. In case of not appropriate tree planting, for example in the Queen's Park Estate where London planes would overwhelm the three-storey Victorian buildings of the estate, trees have been pollarded to just below eaves level. In suburban areas or private gardens, common-sense rules are applied in the same way in planting tree to several meters (at least the house height of distance) from walls to avoid obstruction of windows, damage of roots on water pipes or swimming-pools but also falling trees onto housings. Following these practices, we observe a great shading effect on facades but they generally can't shade roofs both in urban and suburban areas.

Even if some tall trees have been planted without respecting elementary requirements

specifications, it is a statistically very limited design. It could occur mainly in suburban or commercial zones. Places that could be concerned by significant impacts on the energy balance of the roof are places located in low or mid latitude because of a higher sunlight. The potential bias would occur in the early morning or the late evening when the Sun is low on the horizon to allow the shadow cast to reach a significant part of the roof. However, the solar radiation is far lower energetic than around the zenith when the shadow cast can't extend to the roof. So, the potential bias would be very small.

In addition, this process is by far marginal and supposed to have a limited impact on the microclimate within the canyon. Indeed, at 2 meters height, the impact of roof shading on air moisture and temperature could be considered as negligible. Remind that the purpose of this paper is to reduce the uncertainties of the prediction of the impact of urban planing (including greening) on thermal comfort of pedestrians.

Regarding these widespread practices and physical elements of discussion, the implementation of the process of shading of trees on roofs was not a priority for our team but remains technically a feasible project.

We added further explanations in the paper page 6-7, at lines 30-32, 1-8.

Bibliography:

- “Cahier de l'espace public, Chapitre II: Les arbres d'alignement”, Mairie de Toulouse, 2008 (in French)
- “Street tree Management in Barcelona”, Barcelona City Council, 2011 (in French)
- “Streets for all: A guide to the management of London's streets”, Historic England, 2000
- “Buildings height in the Royal Borough”, Royal Borough of Kensington and Chelsea,
- “British Standard 5837: Trees in relation to construction — Recommendations”, British Standards Institution, 2005
- “Trees and the Public Realm (draft version)”, City of Westminster, 2009

5. *“ Page 16, Lines 9-10. The use of the words ‘good’ and ‘only’ are very subjective. You need to state what is it good relative to? ”*

We agreed with the comment of the Referee and reformulated the interpretation of the results.

See in section 6.3 the revisions in the paper.

6. *“ Section 6.4. This section on sensitivity to vegetation layout characteristics and associated figures is not particularly clear. Statements are made without the use of statistical values nor clear comparison using examples from the relevant figures (Figs 8– 10). Page 16 Line 19 states ‘The comparison of statistical scores’, these statistics need to be presented within the text or in a table. ”*

Since we have not highlighted any significant and systematic patterns by studying the effect of tree horizontal coverage, tree canopy height, and tree location, we propose to remove this section which does not bring additional interesting information (as well as associated figures 8, 9, 10).

7. *“ Section 6.4. Figures 8, 9 and 10 do not show any particular clear patterns (there is a lot of scatter and points on top of each other) that allow the reader to determine the full impact of differences in vegetation or whether it was significant, an alternative method for showing this data is required. It is unclear of the utility of comparing two types of error (RMSE and %Err). Could you clarify why you have done this and how this shows how sensitive the model is to these changes? An explanation of this is required in the text. ”*

See response to comment 6.

8. “ *Section 6.5, Figure 11. There are four aspect ratios presented in figure 11 what is the difference between $h/w = 2$ and $h/w = 2b$? The second is not referred to in the text nor the figure caption. ”*

We acknowledge that our paper did not provide sufficient explanations about these additional cases, referred as “ $h/w=2b$ ” in the former version and referred now (in the updated version) as “ $h/w=2$ rescaled vegetation”. These cases show identical urban morphology than classical $h/w=2$ cases but vegetation layer is doubly thicker and higher than $h/w=0.5$ and $h/w=1$ cases for each vegetation configurations in order to rescale it for higher buildings and verify the effect of adapted vegetation layouts regarding to the typology of the street (Cf Fig. 02 and section 5.2.1).

We hope that the readers will find clearer presentation of $h/w=2b$ cases in page 12, at lines 20-24.

9. “ *Appendix A. Why is the view factor between the road and the tree = 0? Surely this would have an implication when calculating the canyon longwave radiation balance as the road will see the underside of the tree layer. ”*

In the updated version of the paper, the view factors are based on the equations of sky view factors in Masson, 2000. Those related to the high vegetation are defined on all the directions. In this way, the interactions between all the facets of the canyon, the sky and trees are allowed in Eq. A6, A7, A8. It ensure the compatibility with the calculations of the longwave exchanges, for which the same view factors but no coefficients are involved. In addition, specific coefficients are applied, in the shortwave scheme only, to constrain the reflections from the high vegetation toward sky and top part of walls. In nature, the solar radiation is mainly redirected upwards by the receiving face of sunlit leaves in the top of crown during the first reflection. We suggest here to neglect the small amount of shortwave radiation which the tree stratum is supposed to reflect to the low part of the canyon during multiple reflections in favor of representing realistically the upward first reflection of solar radiation, which is by far the most energetic reflection.

See page 10, at lines 26-28 and page 11 lines 1-5 the revisions in the paper.

Part 2 : Grammatical and Format Errors

1. “ *TITLE. The authors may wish to amend the title to read more clearly as ‘Implementation of street trees within the solar radiative exchange parameterization of TEB in SURFEX v8.0’. ”*

We changed the title in accordance with the suggestion of the Referee.

2. “ *ABSTRACT, Line 1. With the first use of an abbreviation the term/phrase/name it is used to abbreviate should be stated e.g. Town Energy Balance (TEB) or TEB (Town Energy Balance). The same applies to SOLENE. ”*

We changed the first mention of TEB to “Town Energy Balance (TEB)” in the abstract page 1 line 1 and in the text, page 2 line 22. According to the team who created SOLENE, the name has no official meaning and it is not an acronym. Nevertheless, they inform me of a defined way of typing the name with capital letters and using a smaller font size for the 'OLENE' part, consistently with previous papers.

3. “ *ABSTRACT, Line 3. The word ‘obviously’ is not required here as it is not obvious without reading the paper that there is increased complexity. It would be more appropriate to state this as a fact by removing the words ‘has obviously’.* ”

We removed the expression 'has obviously' in accordance with the suggestion of the Referee (page 1 line 3).

4. “ *Page 2, Line 34. ‘Surimpose’ should read ‘superimpose’.* ”

We corrected this typing error (page 2 line 35). According to the suggestion of the second Referee, we replace 'superimpose' by 'shade' in all the text in order to avoid confusion with contacting surfaces (see comment n°4, part 2 in the section of the second Referee comments).

5. “ *Page 5, Line 13. The work ‘especially’ is not required in this sentence.* ”

We removed this word.

6. “ *Page 6, Line 32. Should the word ‘refined’ be ‘defined’?* ”

We corrected this typing error (page 7 line 10).

7. “ *Page 7, Lines 7 -10. This paragraph is not clear. Should it read as follows? "In order to calculate these terms in TEB, the following section describes how direct solar radiation reaches canyon surfaces. Then, absorption is obtained by separately resolving the first absorption of total solar radiation on each surface and the sum of absorbed shortwave radiation after infinite reflections within the canyon’.* ”

Thank you for reformulating correctly this paragraph. We changed the paragraph in accordance with the suggestion of the Referee (page 7 line 18-21) and added some details as following : “*In order to calculate these terms in TEB, the 4.1 and 4.2 sections describe how direct and diffuse solar radiations reach canyon surfaces. Then, absorption is obtained by separately resolving the first absorption of total solar radiation on each surface and the sum of absorbed shortwave radiation after infinite reflections within the canyon.*”.

8. “ *Page 11, Line 21. Should the first word be TEB on this line?* ”

We corrected this typing error.

9. “ *Page 12, Line 15. This first sentence doesn't read well. Consider splitting into two sentences, one explaining that TEB was run with equivalent configurations and another stating the differences between models.* ”

Thank you for this suggestion. We simplified the sentence (page 13, line 7-8) as following : “*In the same way, the TEB model is run for equivalent configurations to SOLENE configurations, respecting hypotheses, approaches, and spatial resolutions differences between the two models.*”.

10. “ *Page 13, Line 15. Use of the word ‘The’ is redundant in this sentence. Start with ‘Table 3 presents’.* ”

We changed the sentence (page 14, line 21) in accordance with the suggestion of the Referee.

11. *“ Page 13, Line 20. ‘Let’s remind’ is not the correct style nor grammatically correct (Let’s = Let is. If using this use ‘Lets’). You may consider the following change to the sentence. ‘Considering that the temperate climate is characterized by four distinct seasons with contrasting sunshine, air temperature and humidity conditions, seasonal analysis was undertaken’. ”*

We changed the paragraph (page 14, line 28-29) in accordance with the suggestion of the Referee.

12. *“ Page 14, Line 27. Incorrect style and grammar using ‘let’s remind’. The word ‘considering’ would be more suitable. ”*

We corrected the sentence (page 16, line 1) in accordance with the suggestion of the Referee.

13. *“ Page 14, Lines 27-28. This sentence doesn’t make sense. ”*

Thank you for pointing out this misuse of “Inversely”. We reformulated the paragraph section 6.2.

14. *“ Page 16, Line 5. I am not sure what you mean by ‘inversely slightly underestimated’? ”*

Thank you for pointing out this misuse of “inversely”. We reformulated the paragraph section 6.3.

15. *“ Page 16, Line 20. Misspelt ‘exchanges’ ”*

We corrected this typing error (but the section has been removed).

16. *“ Page 17, Line 9. A missing paper reference at the end of this line. ”*

We corrected the .bib file.

17. *“ Page 17, Lines 9-10. Acronyms for models without full model names (as in point 2). ”*

We added the full names of the cited models page 19, lines 17-18.

18. *“ Page 20, Line 2. Missing equation reference. ”*

We corrected the .tex file.

19. *“ Page 22, Line 1. Misspelt ‘example’. ”*

We corrected this typing error.

20. *“ Figures 4 and 6. The shades of blue used to represent ‘wall A’, ‘wall B’ and ‘walls’ are not clear and will not reproduce well if printed in black and white. Consider changing colours or using different line thickness. The subplots are also too small, consider reducing white space between subplots. This could be achieved by limiting the number of axis labels especially as you are using the same scale and variable on each row. ”*

Thank you for these suggestions. We changed the colors and untitled the axes of figures 4 and 4 to allow the reduction of white space between subplots in accordance with the suggestion of the Referee. We hope that description and cited units in captions are enough to understand the figures.

REFEREE 2 :

PART 1 : Major comments

1. “ **English.** Ideally, the English should be edited by a native English speaker. ”

After the revision process and following proofreading we hope that the English is more understandable.

2. “ **Error in application of Beer’s law.** Equations 3-5 appear to be mixed up. Eq. 4 with albedo removed should be the transmission; Eq. 3 as written is the intercepted radiation (multiply it by scattering coefficient to equal scattered radiation); Eq. 5 should be modified accordingly. Please check your model implementation carefully to ensure that it is correct according to the updated equations, and redo the simulations if the model equations were incorrect. ”

Thank you for pointing out these errors. We corrected the equations 3, 4 and 5, page 8, in the paper. The coded equations were already correct but we run new simulations with the different way to code the option of upwards reflections from the high vegetation using classical view factors and specific coefficients in the shortwave radiation scheme (see response 3 and 9, part 1 in the response of the Referee 1, section 4.4 and Appendix A for further explanations). In addition, some adaptations about the calculation of the attenuation in TEB model have been done for the comparison exercise (see section 5.2.2.). SOLENE applies for each vegetation envelope mesh the same 'full' attenuation of 0,5 (assuming that it replace the exponential expression above including the Leaf Area Index). In this way, at each attenuation process, the vegetated meshes in SOLENE attenuates 50% and transmits 50% of the received radiation. Where the Leaf Area Density is involved in the TEB equations (see Eq. B1, B2, B3, B4), we replaced the exponential term by the expression $1 - 0,5(LAD/LAI)$ to express the transmissivity by modulating the theoretical maximum attenuation of 0,5. Considering the LAD likely to be crossed by rays, we can obtain a transmissivity greater than 0,5 with TEB model. On the opposite, SOLENE can not take into account the layer of leaves where the rays are going through and always apply a full attenuation. The hypotheses of the two models are divergent and results have to be interpreted in the light of this divergence. The authors have amended the text in accordance with the suggestion of the Referees and adapted it to the results of the new simulations.

3. “ **Neglect of forward scattering.** From Eqs. 3-6, it appears that forward scattering of intercepted radiation by vegetation is neglected (see Campbell and Norman 1989 for more detail; also, consider revising lines 7-8 on p. 10). Perhaps the albedo and extinction of the foliage are/can be adjusted to account for this. Either way, please explain and/or justify more fully. Can you assume all scattered radiation is scattered upward without introducing significant error? The broadband scattering coefficient is on the order of 0.50 for the leaves of many trees, and approximately 50% of this is forward scattered – so forward scattering potentially represents 25% of the shortwave radiative energy (very approximately). Interception by lower leaves of radiation forward scattered by upper leaves increases total absorption by tree foliage, which may correct the underestimation you find. ”

Thank you for this very interesting comment. We acknowledge that our paper did not provide sufficient explanations about how TEB treats the forward scattering.

As shown in Eq. 2, the direct solar radiation flux potentially received by the high vegetation can be

divided into three components: the transmitted part, the reflected part and the absorbed part. In the code, this potential flux reaching the high vegetation is calculated following the Eq. 1 (see page 7, lines 26-28).

For backward scattered (Eq. 4) and absorbed (Eq. 5) fluxes by high vegetation we use the potential received flux (Eq. 1) corrected by the transmitted part (using $x (1 - \exp(-k \text{LAI}))$ in the classical equation or $x 0.5$ in the comparison cases) in order to obtain the part of the incident flux which theoretically reaches only the leaves in the fraction of high vegetation (in other words, holes within the crown have been removed at this stage). In this way, TEB treats the forward scattering of the incident direct solar radiation flux by the high vegetation. Eq. 10 shows that the diffuse solar radiation flux reaching the high vegetation is also corrected by the transmitted part (page 9, lines 17-18). Indeed, we consider that the available flux, deduced subtracting the fluxes received by the other facets of the canyon (using view factors) from the incident diffuse solar radiation, reaches the high vegetation.

The forward scattering computed at infinite reflections between surfaces of the canyon in shortwave radiation is expressed by the tau terms (Eq. B1, B2, B3, B4). These supplementary elements demonstrate that the forward scattering is not neglected during all the processes occurring in the shortwave radiation scheme.

Concerning the backward scattering from the high vegetation, we suggest here to neglect the small amount of shortwave radiation which the tree stratum is supposed to reflect to the low part of the canyon during multiple reflections in favor of representing realistically the upward first reflection of solar radiation, which is by far the most energetic reflection (see Appendix C).

View factors related to high vegetation are based on the height of the middle of the crown (see Appendix A). In this way, the interception by leaves is assumed to be maximum at this level, so the forward scattering within the crown (on the tree fraction) is allowed to this limit. Explicit interactions from leaves to leaves inside the tree crown are not computed in the current version of TEB.

4. “ Robustness of SOLENE as evaluation tool. How accurate are the SOLENE calculations of solar absorption and scattering by trees? p. 11, lines 7-8: Treatment of foliage in the SOLENE should be further discussed, as well as any associated evaluation, given that this treatment is what TEB is being compared to. Details are sparse in Robitu et al. (2006). Does it include forward scattering, multiple reflection between tree foliage and the urban canyon underneath, or between different tree foliage elements, for example? Differences in model geometries between TEB and SOLENE are discussed; how different are the physics? ”

SOLENE model can simulate the radiative budget of a urban scene represented as a numerical mock-up with explicit vegetation layouts where each mesh is associated to a view factor. Sections 5.2.1 and 5.2.2 have been complemented.

The forward scattering is represented by roughly transmitting 50% of the 'incident' (reaching) flux on the vegetation envelope at the first contact and not a second time when leaving the same envelope by side or toward the ground. Thus, the trees envelopes are considered as semi-transparent.

Multiple reflections are calculated by the radiosity method between all surfaces including tree foliage and the urban canyon underneath or between different lines of crowns. A crucial difference

between TEB and SOLENE is the potential interaction between line of crowns. In TEB, we compute a cumulative fraction of high vegetation. In this manner, interactions between tree lines are not taken into account. On the contrary, in SOLENE, when a ray is intercepted a first time by a vegetation envelope and passed through to reach a second envelope, the ray is attenuated a second time (for example for the vegetation layouts (B3, C3, C4). In this way, an horizontal ray crossing twice a vegetated envelope is attenuated in order to release only 25 % of the initial flux when the rays are leaving the second envelope. Additionally, unlike in SOLENE, the attenuation can be modulated in TEB, respecting the surface-surface interaction considered using the Leaf Area Density (see response 2, part 1).

Finally, the multiple reflections are treated in different ways. In TEB the reflections of shortwave radiation are computed in an isotropic way (see Appendix C) while they are represented as specular reflections in the SOLENE model, using the method of radiosity.

These divergences on the modulation of the attenuation and on the nature of the reflected radiation could partly explain the differences between the received and absorbed solar radiation fluxes of the high vegetation from the two models, apart from the geometrical assumptions.

5. “ Large overall albedo difference. The large differences in mean albedo for higher H/W canyons in Fig. 11 are worrying, and suggests to this reviewer than one or more assumptions made in the formulation in the TEB model are inadequate (assuming the SOLENE model is robust – to point 4 above). It could relate to one of points 2 or 3 above. My sense is that tree foliage limited to the canyon should become less important as H/W increases – if that is true, why would performance degrade? Could this be an issue with the TEB shortwave radiation scheme without trees? A primary purpose of TEB is to provide neighbourhood-scale fluxes to the overlying atmospheric model, and overall albedo is the parameter to which the energy balance is often most sensitive. Hence, this result requires more investigation. ”

Thank you for this very interesting comment. As explained in the previous response, the calculations of the multiple reflections within the canyon between SOLENE and TEB model are too divergent to allow an accurate comparison of absorbed fluxes. For this reason, we changed the figure presenting the mean daily canyon albedo (Fig. 9) in order to represent the comparison of canyon albedos between the simulations of the reference and current TEB version. The results are in line with our expectations, as discussed in the section 6.4.2.

Part 2 : Minor comments

1. “ p. 1, line 8: “...uncertainties in terms of the solar radiative exchanges, as quantified by comparison of TEB...” ”

Thank you for this better reformulation. We corrected the text (page 1, line 8) in accordance with the suggestion of the Referee.

2. “ p.1, line 18: remove “soil artificialisation due to” ”

Thank you for this better reformulation. We corrected the text in accordance with the suggestion of the Referee.

3. “ p.1, line 22: refresh, or cool, clean/filter, etc? ”

Thank you for pointing out this error. We corrected the text (page 1, line 24) with a more suitable term ('these processes cool').

4. *“ p. 2: “surimpose” is not a word I don’t think – do you mean “shade”? And again, p. 6, line 18 I think “shade” or a similar word (obscure?) might be better than “superimpose” (please check throughout). ”*

Thank you for pointing out this typing error (page 2, line 35). We have chosen the term 'superimpose' in the previous version to express the fact that the high vegetation is located above the ground-based surfaces (road and low vegetation). Indeed, this term could be confusing because the low and high vegetation are not in contact. We amended all the text in accordance with the suggestion of the Referee, using the 'shade' term.

5. *“ p. 3, line 2: “...by a microscale radiation model: SOLENE...” ”*

Thank you for this better reformulation. We corrected the text (page 3, line 2) in accordance with the suggestion of the Referee.

6. *“ p. 3, line 12: Krayenhoff et al (2014) ”*

Thank you for pointing out this error. We corrected the reference (page 3, line 13) in accordance with the suggestion of the Referee.

7. *“ p. 4, line 4: “...radiative (Krayenhoff et al. 2014) and dynamic (Krayenhoff et al. 2015) effects...”;
the reference for BEP-Tree is “Krayenhoff (2015)” at present. ”*

Thank you for pointing out this error. We corrected the references (page 4, line 6) in accordance with the suggestion of the Referee.

8. *“ p. 4, line 6: “...both within and above the canyon and above roofs.” ”*

Thank you for these supplementary details. We corrected the text (page 4, line 8-9) in accordance with the suggestion of the Referee.

9. *“ p. 4, lines 14-19: There are some significant assumptions in the view factor calculations and radiation exchange in ENVI-met that could be discussed. However, since it is a microscale model, it may not be relevant to go into much detail. ”*

Thank you for this very interesting comment. We agree with the comment of the Referee and shortened the description of the ENVI-met model (page 4, lines 15-18).

10. *“ p. 4, lines 28-29: I suggest beginning the paragraph as follows: “At each mesoscale model grid point, TEB describes the average characteristics of the local environment by a single urban canyon...” ”*

Thank you for this better reformulation. We corrected the text (page 4, line 25) in accordance with the suggestion of the Referee.

11. *“ p. 8, line 6: This assumes tree foliage is uniformly distributed across the canyon, if I*

understand correctly? If so, this is worth stating in the text. ”

Thank you for this very interesting comment. We acknowledge that our paper did not provide sufficient explanations about how the processes of interception and transmission of the high vegetation are computed respecting the cover fraction approach. For example, Eq. 1 (page 7 lines 29-30) calculates the direct solar radiation flux potentially reaching the high vegetation, considering the height of trees only. So, it express the flux available at this height, corrected by the shading effects of the walls. In further calculations, we associate the fluxes related to the high vegetation (as the reflected and the absorbed ones) to the high vegetation fraction (Eq. 6, Eq. 7). That means that the tree foliage is assumed uniformly distributed across the canyon in Eq. 1 (page 8, lines 20-21), as highlighted by the Referee.

12. “ p. 11, lines 3-6: Is this relevant, if TEB assumes an isotropic distribution? Presumably the same is chosen in SOLENE? ”

Thank you for this very interesting comment. At lines 21-26, page 13, we precise that TEB model is forced with the same conditions of incoming solar radiation than those calculated for the roofs in the SOLENE model. We add a missing element at lines 4-5, page 13: SOLENE has been parameterized to generate perfectly clear cloudless skies. Using a unique forcing for each component (direct or diffuse) of the solar radiation from the SOLENE simulations, TEB forcings do not take into account the non-uniform distribution of incoming diffuse solar radiation on walls. From this imprecision result differences from 1% to 4% between fluxes of the two walls, depending on their orientation, for studied aspect ratios during summertime. Note that an option also allows to represent a non-uniform distribution of the incoming diffuse solar radiation in TEB model but it was deactivated for this experiment.

13. “ Eq. 19: RMSD (difference, not error; since you are comparing two models); also note the critiques of RMSD relative to MAE (Mean Absolute Error), e.g. Willmott et al. 2009. I suggest calculation of MAE instead. ”

Thank you for this excellent suggestion. We have noted the advantages of using the Mean Absolute Error to quantify the mean error instead of the Root Mean Square Error in our study. Consequently, we present the results of MAE in the updated version of our paper, in accordance with the suggestion of the Referee.

14. “ p. 17, line 9: Reference missing. ”

Thank you very much for pointing out this error. We corrected the .bib file.

15. “ p. 26, line 27: Year is 2015, not 2014. ”

Thank you very much for pointing out this error. We corrected the .tex file.

16. “ p. 26, line 29: Year is 2014, not 2013. ”

Thank you very much for pointing out this error. We corrected the .tex file.

17. “ Appendix A, line 1: Eq. ??; and again line 16 on p. 21. ”

Thank you very much for pointing out this error (page 22, line 2). We corrected the .tex file.

18. “ Appendix A, line 19: View factor from road to trees is zero??? Please explain! ”

In the updated version of the paper, the view factors are based on the equations of sky view factors in Masson, 2000. Those related to the high vegetation are defined on all the directions. In this way, the interactions between all the facets of the canyon, the sky and trees are allowed in Eq. A6, A7, A8. It ensure the compatibility with the calculations of the longwave exchanges, for which the same view factors but no coefficients are involved. In addition, specific coefficients are applied, in the shortwave scheme only, to constrain the reflections from the high vegetation toward sky and top part of walls. In nature, the solar radiation is mainly redirected upwards by the receiving face of sunlit leaves in the top of crown during the first reflection. We suggest here to neglect the small amount of shortwave radiation which the tree stratum is supposed to reflect to the low part of the canyon during multiple reflections in favor of representing realistically the upward first reflection of solar radiation, which is by far the most energetic reflection.

See section 4.4 the revisions in the paper.

19. “ Appendix A, line 8: LAD is in m² of leaf area per m³ of volume. ”

Thank you very much for pointing out this error. We corrected the text page 23, line 8.

Implementation of street trees ~~in~~ within the solar radiative exchange parameterization of TEB in SURFEX v8.0

Emilie Redon^a, Aude Lemonsu^a, Valéry Masson^a, Benjamin Morille^b, and Marjorie Musy^b

^aCNRM UMR 3589, Météo-France/CNRS, Toulouse, France, 42 avenue Gaspard Coriolis, 31057 Toulouse cedex 1, France

^bEcole nationale supérieure d'Architecture de Nantes, UMR 1563, quai François Mitterrand, 44262 Nantes cedex 2, France

Correspondence to: A. Lemonsu (aude.lemonsu@meteo.fr)

Abstract. The ~~TEB-Town Energy Balance (TEB)~~ model has been refined and improved in order to explicitly represent street trees and their impacts on radiative transfers: a new vegetated stratum on the vertical plane, which can ~~superimpose to road and shade the road, the walls and the~~ low vegetation has been added. This modification ~~has obviously complexified the~~ led to more complex radiative calculations, but has been done with a concern to preserve a certain level of simplicity and to limit the number of new input parameters for TEB to the cover fraction of trees, the mean height of trunks and trees, their specific Leaf Area Index and albedo. Indeed, the model is designed to be run over whole cities, for which it can simulate the local climatic variability related to urban landscape heterogeneity at the neighborhood scale. This means that computing times must be acceptable, and that input urban data must be available or ~~quite~~ easy to define. This simplified characterization of high vegetation necessarily induces some uncertainties ~~on in terms of the~~ solar radiative exchanges, ~~that were quantified through the as quantified by~~ comparison of TEB with a high spatial-resolution solar enlightenment model (~~SOLENE~~SOLENE). On the basis of an idealized geometry of urban canyon with various vegetation layouts, TEB is evaluated regarding the direct and diffuse solar radiation received by the elements that compose the canyon, ~~as well as the total shortwave radiation absorbed (after multiple reflections) by these elements. The cases of vegetationless canyons lead to root mean square errors less than 15 W m⁻² and biases less than 5 W m⁻². For the cases with high vegetation, the statistical scores are degraded (with a trend of underestimation of solar absorption by trees) but remain acceptable. It is interesting to emphasize that the summertime TEB simulations gave the best scores ($|bias| < 20 \text{ W m}^{-2}$). TEB simulations in summer gathered best scores~~ for all configurations and surfaces considered, which is precisely the most relevant season to assess the cooling effect of deciduous trees under temperate climate. Biases less than $\pm 1 \text{ W m}^{-2}$ related to the direct and diffuse solar radiation fluxes received by road and vertical surfaces have been recorded for vegetationless canyons. Concerning the vegetated canyons we noted a high variability of statistical scores depending on the vegetation layout. The greater uncertainties are found for the solar radiation fluxes received by the high vegetation. The Mean Absolute Error averaged over the vegetation configurations during summertime is $17.27 \pm 9.31 \text{ W m}^{-2}$ for the direct component and $3.45 \pm 1.93 \text{ W m}^{-2}$ for the diffuse component but these scores are associated to acceptable biases: $-14.44 \pm 10.60 \text{ W m}^{-2}$ and $-3.21 \pm 2.20 \text{ W m}^{-2}$, respectively.

1 Introduction

For counteracting the adverse environmental effects that can result of continuous process of ~~soil artificialisation due to~~ urban expansion, numerous projects of local urban planning or design support and favor today the preservation and reintroduction of vegetation in the city. From an environmental point of view, the natural soils and vegetation play a important role and bring significant benefits in different sectors (~~Nowak and Dwyer (2007) ; Mullaney et al. (2015)~~)([Nowak and Dwyer, 2007](#); [Mullaney et al., 2015](#)). They act at a microclimate level through the processes of soil water evaporation and of transpiration of plants (Qiu et al., 2013). These processes ~~refresh cool~~ the ambient air (Zhang et al., 2013) and mitigate the effect of Urban Heat Island (~~Feyisa et al. (2014) ; Önder and Akay (2014) ; Alavipanah et al. (2015)~~)([Feyisa et al., 2014](#); [Önder and Akay, 2014](#); [Alavipanah et al., 2015](#)). The high vegetation, especially the street trees in dense urban neighbourhood, create shadow areas that can locally improve the thermal comfort of pedestrians (~~Spangenberg et al. (2008) ; Shashua-Bar et al. (2011) ; Coutts et al. (2015) ; de Abreu-Harbich et al. (2015) ; Joshi and Joshi (2015)~~)([Spangenberg et al., 2008](#); [Shashua-Bar et al., 2011](#); [Coutts et al., 2015](#); [de Abreu-Harbich et al., 2015](#); [Joshi and Joshi \(2015\)](#)) and reduce the radiation penetration in buildings in summer (~~Abdel-Aziz et al. (2015) ; Akbari et al. (1997, 2001) ; Ko et al. (2015) ; Simpson (2002)~~)([Akbari et al., 1997, 2001](#); [Simpson, 2002](#); [Ko et al., 2015](#); [Abdel-Aziz et al., 2015](#)). For some years now, green roofs are implemented more intensively in cities. The cooling effects they induce on air temperature at pedestrian level are lesser than in case of trees or ground-based vegetation but they modify the energy budget at roof level (Taleghani et al., 2016). Nonetheless, they help to reduce the temperature fluctuations of structural roofs and to better insulate buildings (~~Hien et al. (2007) ; Kokogiannakis et al. (2011)~~)([Hien et al., 2007](#); [Kokogiannakis et al., 2011](#)). Many studies highlighted their efficiency to significant energy savings for heating and air conditioning (Jim, 2014). The implementation of pervious soils, whether at the ground or on buildings, also enables a more effective and sustainable management of rainwater, by the storage of water in the soil and the decrease of surface water runoff (~~Armson et al. (2013) ; Yao et al. (2015) ; Zhang et al. (2015)~~)([Armson et al., 2013](#); [Yao et al., 2015](#)). Besides micro climatic and hydrological impacts, the urban vegetation is identified as a biodiversity reservoir for fauna and flora in cities (Alvey, 2006). It also plays its part in architectural atmospheres, and more widely in the perception of environmental quality by the population. The green spaces in urban environment are generally perceived very positively by inhabitants because they are places of wellness, detente, and user friendliness (~~Bertram and Rehdanz (2014) ; Bowen and Parry (2015)~~)([Bertram and Rehdanz, 2014](#); [Bowen and Parry, 2015](#)).

In order to investigate some of the physical processes related to the presence of vegetation in urban environment, e.g. for microclimate, hydrology or building energy ~~consumption~~ issues, the ~~modelling modeling~~ is definitely a necessary tool. It is also pretty relevant and powerful to assess greening strategies by quantifying the potential impacts, and it consequently enables to answer to some important expectations of public stakeholders and urban planners.

The ~~TEB~~ [Town Energy Balance \(TEB\)](#) urban canopy model (Masson, 2000) is today applied for many studies of climate change impacts at city scale. Among the numerous strategies of adaptation to climate change, and attenuation of Urban Heat Island, the benefits of urban environment greening has been investigated through more or less realistic scenarios. Kounkou-Arnaud et al. (2014) and de Munck (2013) have proposed and tested some strategies of ground-based vegetation implementation for the city

of Paris (France). They have evaluated the cooling potential of this vegetation through the evapotranspiration process during summer. They investigated and quantified the impacts in terms of decrease of air temperature inside the streets, as well as improvement of thermal comfort conditions outside and inside buildings. The works of de Munck (2013) have also addressed the issues of building energy consumption and of water resource at ~~pluriannual~~multi-year and seasonal scales.

5

For such ~~modelling exercises, the TEB model~~modeling exercises, TEB had been previously improved in order to explicitly represent urban vegetation within the ~~canyons~~canyon and to parameterize at small-scale the radiative and energetic interactions between the built-up covers and the vegetation (Lemonsu et al., 2012). All types of vegetation are however managed as a ground-based layer: leaves can be in shade of buildings but do not create themselves shadow effects on roads or buildings.

10 With the current developments we attempt to remedy this lack by modifying the solar radiation budget of tree-filled canyons. The tree layer can now ~~surimpose shade~~ ground-based surfaces and walls. In this way, interception, transmission or absorption of solar radiation by this additional non-opaque surface are computed. These implementations ~~will be~~are evaluated by a comparison with simulations provided by a ~~fine-scale model of enlightenment: SOLENE~~microscale radiation model: SOLENE, developed at the CERMA laboratory, Nantes, France.

15 **2 Urban high vegetation** ~~modelling~~modeling

Until recently, very few urban climate models were able to take into account natural soils and vegetation. This fact constitutes a significant limitation in ~~modelling~~modeling the radiative and energetic exchanges in urban environments, according to the results of the intercomparison exercise of urban models performed by Grimmond et al. (2011). Most of models that already included vegetation were based on the tiling approach which consists in dealing separately with impervious covers and natural covers with distinct parameterizations and without ~~micro-scale~~microscale interactions between vegetation and built-up elements. However, an important effort has been conducted these last years in order to improve the representation of physical processes related to the presence of vegetation in urban climate models. Suburban and residential areas are characterized by an abundant vegetation (all types confounded) while ~~they~~trees are predominant in cities. This feature of most of cities have motivated the concern of improving urban ~~micro-climate modelling~~microclimate modeling in such areas.

25 ~~?~~Krayenhoff et al. (2014) present an exhaustive literature review of existing models and their characteristics.

More especially, different approaches are today applied for implementing high vegetation and its implication in calculation of radiative and energetic exchanges. Among following single-layer models with integrated vegetation scheme, Lee and Park (2008) have been the first to deal with effects of trees in urban canyons in their vegetated urban canopy model (VUCM). The foliage layer is explicitly represented in the middle of the canyon above the ground. It is characterized by a cover fraction of the canyon, a thickness, and a vertical profile of Leaf Area Density (LAD). The trunks are assumed to be transparent as it is often the case in vegetation models. Radiation budget is computed for shortwave radiation (direct and diffuse components) by accounting for shadowing effects of trees on buildings and ground-based surfaces and of buildings on trees, as well as multiple

reflections, and for longwave radiation with one reflection. The hypothesis of lambertian reflectance is applied by considering each element of the canyon as a uniform surface (with uniform albedo, emissivity and temperature). For each of them, the view factors in relation to surrounding elements are computed at the center of the surface. The attenuation of radiation by leaves is included in equations when short- or long-wave radiation crosses the foliage. It depends on transmissivity properties of foliage - inspired by works of Yamada (1982) for forest canopies - that follow an exponential law based on the LAD profile and a modulation factor depending on vegetation type. More recently, Young et al. (2015) have ~~implemented~~ developed and tested a similar parameterization for street trees (TUrban) in the ~~Met-Office—Reading Urban Surface Exchange Scheme (MORUSES, ??)~~ Single Column Reading Urban Model (SCRUM, Harman and Belcher, 2006; Porson et al., 2009). The tree canopy is explicitly described as a rectangle located in the middle of the canyon and assumed to be lower than building height. ~~Additional~~ The view factors for both fully visible and partially occluded facets due to the presence of the ~~tree are calculated using an analytical method from Hottel (1954)~~ foliage are calculated in an analytic manner, based on Hottel's crossed string construction (Hottel, 1954). The model implemented by Ryu et al. (2015) considers two explicit and symmetric trees with circular crowns. The Monte Carlo algorithm developed by Wang (2014) is executed once at the beginning of the simulation and subsequently transformed into simple relations to determine view factors which trees are involved. Short- and long- wave radiation exchanges but also sensible and latent heat exchanges and root water uptake processes are represented.

BEP-Tree is the first multi-layer model of urban energy exchange and flow at the neighborhood scale that includes trees and their both radiative (Krayenhoff et al., 2014) and dynamic (Krayenhoff et al., 2015) effects on buildings. View factors are also computed using a Monte Carlo ray tracing approach. The clustered distribution of tree crowns is taken into account through a unique clumping factor for all the vegetation of the canyon. Tree foliage can be present both within and above the canyon and above the roofs.

For large eddy simulations (LES) in urban environment, a vegetated urban canopy model (VUC) has been integrated by Tavares et al. (2015) in the ARPS model. This ARPS-VUC version distinguishes the tree canopy from natural soils and ground-based vegetation. The radiative calculations are however rather simplified in relation to dynamics. The net radiation flux decreases exponentially from the top of urban canopy to the ground depending on the canopy density which includes both tree vegetation and buildings. For a microscale urban climate model such as ENVI-met (Bruse and Fleer, 1998), the fine meshing enables to resolve explicitly each element which composes the urban environment by distinguishing buildings, impervious and natural ground-based surfaces, vegetation, and air. ~~More especially for radiative calculations, short and long wave net budgets can be computed at each grid mesh, by accounting for shadow effects of buildings and absorption by vegetation. For this, a separate sky-view factor is calculated in the middle of each grid mesh, and absorption~~ Absorption coefficients of radiation by vegetation (based on an exponential formulation) are calculated at each vertical level, according to the vertical profile of LAD. ~~The SOLENE-microclimat~~ The SOLENE-microclimat model (based on the ~~SOLENE-SOLENE~~ radiative model) is able to represent the evaporative, shading and insulating characteristics of green walls and roofs, modeled as surfaces (Malys, 2012). The trees are ~~modelled~~ modeled as porous volumes in the airflow model and as semi-transparent crowns in the radiative model; the

energy balance (evaporative, convective and radiative fluxes) being coupled to these models (Robitu et al., 2006). This balance leads to the assessment of leaves and air temperatures.

5 3 General concept of TEB and urban trees representation

3.1 Description of urban areas in TEB

~~The TEB model describes the urban areas on the basis of the urban canyon concept. At the scale of a modelling~~ At each mesoscale model grid point, ~~the mean TEB describes the average~~ characteristics of the local environment ~~are represented~~ by a single urban canyon composed of a ground-based surface bordered by two flat-roof buildings of same height. The urban environment is thus described in TEB based on four distinct elements that compose the urban canyons: *roof*, *wall*, and for the ground-based surfaces, a combination of impervious and natural covers referred to as *road* and *garden*, respectively (Fig. 1).

A set of geometric parameters are defined to describe the canyon (Table 1): cover fractions of buildings and gardens (the remaining fraction is assumed to be the roadways), mean building height, and wall area density. Impervious covers are also characterized by radiative and thermal properties depending on construction materials: albedo and emissivity are prescribed for outdoor surface coating of roofs, walls, and roads; thermal conductivity and heat capacity are defined for the ensemble of materials composing buildings and roadways. For each urban facet (*roof*, *walls* and *road*) separately, the model computes a radiation budget and a surface energy balance. It also resolves an equation of temperature evolution with a single surface temperature associated to each facet.

For natural soils and vegetation, the radiative and energetic exchanges with atmosphere, as well as the hydrological and thermal processes in the ground are parameterized with the Interaction Soil-Biosphere-Atmosphere model (ISBA) model (Noilhan and Planton, 1989). The vegetation stratum is described in the ISBA model as an aggregation of bare soil, low stratum (grass) and high stratum (trees) of vegetation. This vegetation stratum is characterized by composite descriptive and physiologic properties that are calculated starting from properties of these different types of natural covers. They include ~~especially~~ albedo and emissivity (depending of proportion of bare soil and vegetation), Leaf Area Index, stomatal resistance, and roughness length. Note that some of those properties can evolve seasonally, but also in case of snowfall which modifies radiative properties. The vegetation stratum is connected with a soil column (~~Boone et al., 1999~~), to which are associated hydrological and thermal properties depending of soil texture and water content evolution (Boone et al., 1999).

This reference version of TEB is based on two important simplifications. First, there is no explicit spatial arrangement of the ~~gardens within the canyons~~ garden within the canyon. They are only represented as land cover fractions. In addition, the vegetation stratum, even if it can be composed of trees (through the definition of specific physiological properties), is always placed on the ground without vertical extent. This means that shadow effects on ground and buildings related to the presence

of high vegetation are not taken into account, and that there is no vertical distribution of energy turbulent exchanges between vegetation and atmosphere.

3.2 General principles of solar radiation exchange parameterization in TEB

The present study describes the improvements of the radiation budget calculations in TEB by the implementation of explicit high vegetation. Consequently, this section is focused on the description of the radiative exchanges in the initial version of TEB. The parameterization of turbulent heat fluxes and of heat conduction processes, as well as the calculations of microclimate parameters within the canyon, are not presented here (~~see Masson (2000); Lemonsu et al. (2004); Hamdi and Masson (2008); Masson and Seity (2009); Lemonsu et al. (2012) for details~~)but they are detailed by Masson (2000); Lemonsu et al. (2004); Hamdi and Masson (2008); Masson and Seity (2009); Lemonsu et al. (2012) for details

10 The TEB urban canyons are assumed to be of infinite length so that there is no street intersection. The radiative ~~calculation~~ calculations are consequently done on a two dimensional plan which crosses the canyon according to an axis perpendicular to the street direction. Two main options are available for radiative calculations: (1) a street orientation can be prescribed, so that the two walls of the canyon (referred to *wall A* and *wall B*) are managed separately; or (2) the hypothesis of ~~streets-isotropic orientation~~ isotropic orientation of streets is applied, and in this case, walls are managed together (implying that they will have

15 identical temperature evolutions).

The short- and ~~long-wave~~ long- wave radiation budgets are resolved in TEB for each element composing the urban canyon (roofs, walls, road, ground-based vegetation, and now tree canopy) with the aim of determining the energy absorbed by each element, that is used afterward to compute the surface energy budget.

20

~~For a given element, More specifically for~~ the shortwave radiation budget ~~combines three contributions~~, three contributions are considered for a given element:

1. The direct solar radiation received before any ~~reflection~~ reflections. This contribution depends on ~~zenithal~~ zenith angle since the incident direct radiation is unidirectional, street orientation, and canyon aspect ratio.
- 25 2. The diffuse solar radiation received before any ~~reflection~~ reflections. This contribution depends on the ~~sky-view~~ sky view factor of the considered element since the diffuse radiation is assumed to be isotropic.
3. The total shortwave radiation received after multiple reflections within the canyon. After a first reflection on one of the elements of the canyon, initial contributions of direct and diffuse radiation are isotropic and are treated the same way. The part of radiation received by a given element then depends on the view factors of all the other elements and on their
- 30 ~~albedos~~ albedo that determine the reflected radiation part.

Although this paper focuses on resolution and evaluation of the shortwave radiation budget, it is worth to note that the validation of our shortwave radiation scheme contributes to verify our future longwave radiation scheme. Indeed, the same view factors

used for the multiple reflections will be applied to the longwave radiation interactions within the canyon. The longwave exchanges are computed following the typical Stefan-Boltzmann law. Moreover, because of high longwave emissivities, only one re-emission is computed. For numerical stability purpose, an implicit formulation is applied for longwave radiation budgets; it includes the surface temperatures at the previous numerical time step and at the current time step.

5 3.3 Inclusion of a high vegetation stratum for solar radiation calculation

To take into account the tree canopy in TEB, it is required to add a new vegetated stratum on the vertical plane, which can ~~superimpose to road and~~ shade the road, the walls and the low vegetation. This modification ~~obviously complexifies the led~~ to more complex radiative calculations, but is done with a concern to preserve a certain level of simplicity and to limit the number of new input parameters for TEB. ~~It is important to emphasize that the model is designed to be run over whole cities, for which it can simulate the local climatic variability related to urban landscape heterogeneities at the neighborhood scale~~ This is motivated by the type of applications which are conducted with the TEB model, and more generally with the SURFEX land surface modeling platform (Masson et al., 2013) which TEB is part of. The system is frequently applied over domains of several hundred square kilometers with horizontal resolutions between few hundred meters to few kilometers and can be run for long time periods up to several years in case of climatic studies (e.g., Lemonsu et al., 2013; de Munck, 2013, in French).

15 This means that computing times must be acceptable, and that ~~input urban-urban input~~ data must be available or ~~quite~~ easy to define.

The arrangement of tree canopy is here described using three parameters only (Fig. 1 and Table 1): its cover fraction (δ_t), i.e. the proportion of canyon which is covered by the foliage stratum on the horizontal plane, as well as the mean height of trees (h_t), and the mean height of trunks (h_{tk}). ~~Urban~~ In the current version of TEB (official SURFEX v8.0 version), urban trees are assumed to be less tall than surrounding buildings and systematically confined inside the canyon so that they cannot provide shade for roofs. This hypothesis is in accordance with urban planning ~~rules requirements specifications~~ for street trees management ~~; that impose some restrictions relative to the location and height of trees. In case of public parks and private gardens, the trees are usually planted far enough from buildings~~ (in French, Municipality of Toulouse, 2008; City of Westminster, 2009; Barcelona City Council,

25 These documents ensure a satisfactory juxtaposition of trees with urban structures for dwellers. Minimum distances between trunks or crowns and walls or balconies are strictly imposed to avoid problems such as excessive obstruction of crowns facing windows, disruption of underground services by roots or subsidence of buildings. These widespread practices are also applied in private gardens or suburban areas and tends to avoid shadow on roofs even if these street trees can be taller than buildings. Design with trees shading on roofs are statistically sparse and their impact on surface balance limited. They are probably

30 located in high latitudes where incoming fluxes are lesser than in mid or low latitudes and this potential bias would only occur in the early morning or late evening, when the zenith angle is large but the solar radiation flux far lower energetic than around noon.

For now, the shape of the foliage and the vertical distribution of leaves are not ~~refined~~ defined. The crowns of trees are con-

sidered as parallelepipeds (namely computed as a rectangular 2D cross-section) with homogeneous foliage which is described by a Leaf Area Index (LAI_t) and an albedo (α_t). It is however possible to vary the LAI during the year, in order to simulate the seasonal cycle of deciduous trees. Note that trunks are not taken into account in radiative calculations. The tree vegetation stratum is considered as a ~~semi-transparent~~ partially-transparent element for shortwave radiation. A part of the incident radiation received by trees is transmitted through the foliage. The part of radiation which is not transmitted is ~~either~~ consequently reflected or absorbed, depending on albedo. These processes and the associated calculations are detailed hereafter.

4 Solar radiation absorption of vegetated street canyon surfaces

10 In this part, equations related to the implementation of a tree layer into the TEB model are presented. In order to calculate these terms in TEB, the ~~first 4.1 and 4.2~~ following sections describe ~~the way the solar radiation reaches~~ how direct and diffuse solar radiations reach canyon surfaces. Then, absorption is obtained ~~using separated resolings of~~ by separately resolving the first absorption of total ~~solar radiation and~~ shortwave radiation on each surface and the sum of absorbed shortwave radiation after infinite reflections within the canyon.

15 4.1 Direct solar radiation received by each element

The foliage of trees plays a role of obstruction and attenuation of incident direct solar radiation (S_t^\downarrow) for the other elements of the urban canyon. Consequently, to determine the direct solar radiation received by each element of the canyon, we need to solve first the equations related to high vegetation.

20 The direct solar radiation ~~reaching high vegetation~~ potentially reaching the top of trees by geometrically taking into account the shading of buildings depends on buildings height (h), canyon aspect ratio (h/w), street orientation (θ_{can}), ~~zenithal~~ zenith and azimuth angles (λ, θ_{sun}), as well as tree height (~~h_t~~ h_t):

$$h \tan(\lambda) \sin |\theta_{sun} - \theta_{can}| \tag{1}$$

25

As explained previously, this radiation flux is partially transmitted through the foliage (S_t^{\gg}), whereas the remaining solar radiation is reflected (S_t^\uparrow) or absorbed (S_t^*):

$$S_t^\downarrow = S_t^{\gg} + S_t^\uparrow + S_t^* \tag{2}$$

The proportion of direct solar radiation transmitted through the foliage is estimated by a Beer Lambert law (Campbell and Norman, 1989) where the Leaf Area Index (LAI_t expressed in m^2 of leaves per m^2 of ground) of tree canopy and an extinction coefficient (k) are involved. The extinction coefficient is fixed to 0.5, a default value corresponding to homogeneous repartition of leaves in terms of density and orientation (in other words, a spherical leaf angle distribution):

$$S_t^{\gg} = S_t^{\downarrow} \underline{1 - \exp(-k LAI_t)} \quad (3)$$

The reflected radiation part simply depends on the part of incident solar radiation untransmitted through the foliage and on the albedo of trees (α_t):

$$S_t^{\uparrow} = \alpha_t S_t^{\downarrow} \left(\underline{1 - \exp(-k LAI_t)} \right) \quad (4)$$

10 Finally, the incident direct ~~radiation~~ solar radiation part absorbed by trees is neither transmitted nor reflected and calculated as the residual term ~~calculated~~ from Eq. 2:

$$S_t^* = (1 - \alpha_t) S_t^{\downarrow} \left(\underline{1 - \exp(-k LAI_t)} \right) \quad (5)$$

The direct solar radiation received by the ground (indiscriminately road or garden fraction) is deduced by correcting the incident solar radiation above canyon from the interception of radiation by high vegetation canopy (i.e., reflected and absorbed radiation weighted by high vegetation cover fraction referred to as δ_t), and then from the shading effects of buildings (~~according to Lemonsu et al. (2012)~~ according to Lemonsu et al., 2012). The same equations are obtained for road (S_r^{\downarrow}) and garden (S_g^{\downarrow}):

$$S_r^{\downarrow} = \left(S^{\downarrow} - \delta_t \left(S_t^{\uparrow} + S_t^* \right) \right) \max \left[0; 1 - \frac{h}{w} \tan(\lambda) \sin |\theta_{sun} - \theta_{can}| \right] \quad (6)$$

In this way, tree foliage is assumed to be uniformly distributed across the canyon at the height of the trees (h_t), consistently with the Eq. 1.

20

The direct solar radiation which is not received either by high vegetation, or by road or garden is assigned to the sunlit wall, whereas the opposite wall is in the shadow. By convention in TEB in the case of an oriented canyon, we define *wall A* as the most sunlit wall and *wall B* as the shaded one.

$$S_{w_A}^{\downarrow} = \left(S^{\downarrow} - S_r^{\downarrow} - \delta_t \left(S_t^{\uparrow} + S_t^* \right) \right) \frac{w}{h} \quad S_{w_B}^{\downarrow} = 0 \quad (7)$$

25 Note that shading effects of high vegetation on roofs are not represented, since urban trees are less tall than buildings by definition in the current version of TEB (SURFEX v8.0).

4.2 Diffuse solar radiation received by each element

The incoming diffuse solar radiation (S^{\downarrow}) is assumed to emit isotropically. Each urban surface of the canyon (*wall*, *road*, and *garden*) receives a part of diffuse solar radiation according to the sky-view sky view factor of the surface Ψ_* (see Appendix

A) and the mean radiative transmissivity between the sky and the given surface τ_{*s} (see Appendix B). Note that the [sky-view sky view](#) factor of *wall* is defined at mid-height of buildings; for ground-based surfaces *road* and *garden*, a single [sky-view sky view](#) factor $\Psi_{rs} = \Psi_{gs}$ is defined at the center of the street ([Masson \(2000\); Lee and Park \(2008\)](#)) ([Masson, 2000; Lee and Park, 2008](#)). The following equations are obtained for *road* (same expression for *garden*) and for *wall*:

$$5 \quad S_r^\downarrow = S^\downarrow \Psi_{rs} \tau_{rs} \quad (8)$$

$$S_w^\downarrow = S^\downarrow \Psi_{ws} \tau_{ws} \quad (9)$$

We admit that the residual flux of diffuse solar radiation which is not intercepted in the canyon by previous surfaces reaches the tree canopy:

$$10 \quad S_t^\downarrow = \frac{S^\downarrow - (\delta_r S_r^\downarrow + \delta_g S_g^\downarrow + \frac{2h}{w} S_w^\downarrow)}{\delta_t} \quad (10)$$

[This method presents two major advantages: \(1\) the diffuse solar radiation budget is always closed and \(2\) the computed diffuse solar radiation flux for the high vegetation is already corrected from the transmitted part, reaching the other surfaces.](#)

The fluxes of each surface are here expressed according to the total ground-based surface of the canyon, with δ_r and δ_g the cover fractions of road and garden in the canyon ($\delta_r + \delta_g = 1$), respectively.

4.3 First absorption of total [solar shortwave](#) radiation by each element

The first absorption of total [\(direct and diffuse\) solar radiation \$S^*\(0\)\$ shortwave radiation \$S^*\(0\)\$](#) , before any reflections, is only function of the total [solar shortwave](#) radiation received by the considered element and of its albedo (α_*). The same expression is obtained for walls and ground-based surfaces (\star which stands for r, g, w_A or w_B):

$$20 \quad S_*^*(0) = (1 - \alpha_*) (S_*^\downarrow + S_*^\uparrow) \quad (11)$$

For the tree canopy, the part of absorbed direct solar radiation is corrected by the transmitted flux:

$$S_t^*(0) = (1 - \alpha_t) \left[\left(S_t^\downarrow - S_t^{\gg} \right) + S_t^\uparrow \right] \quad (12)$$

S_t^\downarrow includes the transmitted flux [\$S_t^{\gg}\$](#) (see Eq. 2) contrary to S_t^\downarrow which is calculated as a residual flux (Eq. 10), [not intercepted by other surfaces corrected from the transmitted flux.](#)

25 4.4 [Sum of total shortwave radiation absorbed by each element](#)

4.5 [Sum of total solar radiation absorbed by each element](#)

Our goal is to compute the total [solar shortwave](#) radiation absorption for each element $S^*(\infty)$ by taking into account an infinite number of reflections between all elements composing the urban canyon. At each reflection, the isotropic radiation

intercepted by a given element (1) after reflections on one of the other elements (2) is conditioned by the view factor of (2) from (1) referred to as Ψ_{12} (see Appendix A), the mean radiative transmissivity τ_{12} (see Appendix B) and the absorption is then determined according to reflective properties of (1). Using a single view factor in TEB radiation calculations is obviously a limitation for accurately representing the various contributions of canyon's surfaces to high vegetation. Additionally, we have a poor knowledge of a potential contribution of leaves with each others, within the tree's crown. To ensure a closing system, we define the total absorbed shortwave radiation by high vegetation as the remaining shortwave radiation, after accounting for absorption and reflection from the total incident solar radiation by all other elements of the canyon. This requires to calculate the part of shortwave radiation which ~~goes out~~ leaves the canyon towards the sky. The terms R_∞ , G_∞ , A_∞ , B_∞ , and T_∞ make reference to the sum of total solar shortwave radiation reflected by each surface, respectively, after an infinite number of reflections (see detailed resolution in Appendix C). Here is the expression of the total absorbed solar flux per surface:

$$10 \quad S_s^*(\infty) = \Psi_{sr}\tau_{sr}(\delta_r R_\infty + \delta_g G_\infty) + \Psi_{sw}\tau_{sw} \frac{A_\infty + B_\infty}{2} + \Psi_{st}\delta_t T_\infty \quad (13)$$

$$S_r^*(\infty) = S_r^*(0) + (1 - \alpha_r) \left[\Psi_{rw}\tau_{rw} \frac{A_\infty + B_\infty}{2} + \underline{c_{rt}} \Psi_{rt}\delta_t T_\infty \right] \quad (14)$$

$$S_g^*(\infty) = S_g^*(0) + (1 - \alpha_g) \left[\Psi_{rw}\tau_{rw} \frac{A_\infty + B_\infty}{2} + \underline{c_{rt}} \Psi_{rt}\delta_t T_\infty \right] \quad (15)$$

15

$$S_{w_A}^*(\infty) = S_{w_A}^*(0) + (1 - \alpha_w) \left[\Psi_{wr}\tau_{wr} (\delta_r R_\infty + \delta_g G_\infty) + \Psi_{ww}\tau_{ww} B_\infty + \underline{0.5c_{wt}} \Psi_{wt}\delta_t T_\infty \right] \quad (16)$$

$$S_{w_B}^*(\infty) = S_{w_B}^*(0) + (1 - \alpha_w) \left[\Psi_{wr}\tau_{wr} (\delta_r R_\infty + \delta_g G_\infty) + \Psi_{ww}\tau_{ww} A_\infty + \underline{0.5c_{wt}} \Psi_{wt}\delta_t T_\infty \right] \quad (17)$$

$$20 \quad S_t^*(\infty) = \frac{1}{\delta_t} \left[\left(\left(S_t^\downarrow - S_t^{\geq} \right) + S_t^\downarrow \right) - \left(S_s^*(\infty) + \delta_r S_r^*(\infty) + \delta_g S_g^*(\infty) + \frac{2h}{w} \frac{S_{w_A}^*(\infty) + S_{w_B}^*(\infty)}{2} \right) \right] \quad (18)$$

~~It seems reasonable to presume that at the first reflection,~~

The view factors related to the solar radiation is mainly redirected from the leaves to the sky or to the high vegetation stratum are expressed in Appendix A. Specific coefficients are applied, in the shortwave scheme only, to constrain the reflections from the high vegetation toward sky and top part of walls seen by leaves. On the contrary, the multiple reflections occurring within the canyon are computed in an isotropic way. Though reflections can have different behaviors, we use a single view factor for each pair of surfaces. Our purpose is, In nature, the solar radiation is mainly redirected upwards by the receiving face of sunlit leaves in the top of crown during the first reflection. We suggest here to neglect the small amount of shortwave radiation which the

25

~~tree stratum~~ is supposed to ~~be reflected by the high vegetation stratum towards the~~ reflect to the low part of the canyon during multiple reflections ~~, but to favor a realistic representation of the first upward~~ in favor of representing realistically the upward first reflection of solar radiation ~~by trees. In Appendix A the view factors linked to the high vegetation stratum are expressed for both options, and their impact on solar~~, which is by far the most energetic reflection. Solar reflections calculations are fully explained in Appendix C. As previously mentioned, view factors used for the multiple reflections in the shortwave radiation scheme will be applied to the longwave radiation interactions within the canyon in future works.

5 Comparative exercise with the ~~SOLENE~~ SOLENE model

5 An objective and exhaustive assessment of the new solar radiation calculations in TEB related to the inclusion of tree layer effects is not an easy exercise, essentially due to the lack of experimental data. Indeed, very few measurements for documenting radiative effects of trees in urban environment are available (Park et al., 2012). The objective is here to quantify the performances of TEB in simulating the different contributions of the solar radiation budget for the ensemble of urban facets and vegetation. For this purpose, we compare TEB with the ~~SOLENE~~ SOLENE software, which is a high spatial-resolution solar and lighting architectural model and which is used in this ~~ease-work~~ as a reference. Various configurations of urban canyons with street trees (that differ in terms of vegetation density and spatial distribution) are studied so that the capacities and limits of the TEB geometric approach can be highlighted and evaluated.

5.1 General presentation of the ~~SOLENE~~ SOLENE model

15 The ~~SOLENE model (Miguet and Groleau (2002); Robitu et al. (2006); Groleau and Mestayer (2013))~~ SOLENE model (Miguet and Groleau (2002); Robitu et al. (2006); Groleau and Mestayer (2013)) is a radiative transfers scheme based on the radiosity method which is applied to meshed scenes with triangular facets, particularly adapted to complex geometries (~~Bouyer et al. (2011); Malys et al. (2014))~~ (Bouyer et al., 2011; Malys et al., 2014). This model provides a good tool to study urban radiation distinguishing solar radiations (separate direct and diffuse components, 0.3-2.5 μm) and infrared thermal radiations (2.5-18 μm).

20 In this research work, ~~only solar radiations are considered~~ we consider the shortwave radiation scheme only. The incoming direct solar radiation is calculated by considering the sun as a point source, related to solar height (following formula in De Brichambaut (1963)) and angle of incidence of rays at the surface (Miguet, 2000). The incoming diffuse part of solar radiation is represented as a non-uniform distribution coming from a sky vault defined by an hemisphere of infinite radius, which is meshed using a geodesic triangulation. The luminance values that are mapped on the hemisphere are derived from Perez model (Perez et al., 1993). This model, based on five sky clearness and ~~sky~~ brightness, provides statistical distribution depending on weather type represented. Multiple reflections are computed assuming that the surfaces are lambertian and opaque for urban surfaces while the vegetation surfaces are semi-transparent ~~according to their Leaf Area Density~~ (Robitu, 2006). Solar simulations are performed in successive stages. The first one, based on geometric procedures, determines the visibility considering solar masks between two mesh elements or a mesh element and a sky patch of the sky vault model (including sun). View factors

30 (including sky view factor) are produced for each mesh. The second stage calculates the solar radiation [fluxes](#) received by each mesh element for the time-step. Then, the multiple reflections are computed by the radiosity method. This last stage provides the net solar flux received by each mesh as well as absorbed and reflected parts.

The trees have been implemented from the evolution of [SOLENE-SOLENE](#) into the microclimate model named [SOLENE-microclimat](#) [SOLENE-microclimat](#) (Robitu, 2006). In this new model, the trees are geometrically modeled by their external envelope and are considered as semi-transparent. Therefore, a percentage of the solar radiation is transmitted by the tree canopy according to a transmission coefficient ([fixed to 0.5](#)) and reaches other elements of the urban scene.

5 5.2 Configuration of numerical experiments

5.2.1 Canyon ~~modelling~~ modeling in [SOLENE-SOLENE](#)

The urban canyon geometry chosen for building the [SOLENE-SOLENE](#)'s mock-ups is as simple as possible to reflect the hypotheses of [TbriehambautEBTEB](#): an infinite street (150 m in length in the mock-ups) bordered by two identical buildings with flat roofs. As shown in Fig. 2, it is declined in three different urban canyon forms corresponding to aspect ratios (referred to as h/w) of 0.5, 1 and 2. For the first two ~~canyons~~ [aspect ratios](#), the building height is 8 m and the width of the street is 16 m for $h/w = 0.5$ and 8 m for $h/w = 1$. For $h/w = 2$, building height is 16 m and width of the street is 8 m.

For each of these urban canyons, 13 different vegetation layouts are prescribed (Fig.3), as well as a control case without vegetation. The vegetation blocks are parallelepipeds representing the three-dimensional tree crowns, without trunk. The vegetation blocks are continuous lengthwise the canyon. Depending on the configurations, the trees can be organized in single or double rows. According to a cut plan through the canyon, the tree crowns can fill 30, 60, or 90 % of canyon width. For the three aspect ratios, height of trees is prescribed to 5 m or 7.5 m with trunks of 2.5 or 5 m, so that the thickness of tree canopy varies between 2.5 and 5 m. ~~An additional configuration is tested for aspect ratio~~ [Additional configurations \(referred to as \$h/w = 2\$; for rescaled vegetation\)](#) are tested for which height of trees is prescribed to 10 m or 15 m with trunks of 5 or 10 m, ~~depending on the thickness and the location of the crown (Cf. Fig. 2). In other words, vegetation layer is doubly thicker and higher than $h/w = 0.5$ and $h/w = 1$ cases for each vegetation configuration in order to rescale it for higher buildings and verify the effect of adapted vegetation layouts regarding the typology of the street.~~ For all experiments, the [LAI-Leaf Area Index](#) of trees is prescribed to 1, and the albedo is prescribed to 0.25 for road, 0.30 for walls, and 0.25 for trees. All configurations are described in Fig. 1, 2, 3 and Table 2.

25

To treat the ensemble of configurations, 55 digital mock-ups (52 canyons with vegetation and 3 canyons without vegetation) have been built with the computer-aided-design (CAD) Salome V7_4_0 software. All mock-ups have been meshed by the GMSH software which is a finite element mesh generator. We have applied here a non-uniform meshing [with a characteristic length of only 1 m](#) in order to refine the spatial discretization of vegetation blocks, whose smallest ones for some of the vege-

30 tation layouts do not exceed 2.4 m of width and 2.5 m of height.

Each canyon is projected following the four street orientations 0° , 45° , 90° , and 135° (degrees from geographical north, in the counter trigonometric direction). A specific location (defined by latitude and longitude) must be prescribed for astronomic calculations. The city of Nantes (France) is chosen in an arbitrarily manner (46° N, 1° E). The solar radiation exchanges are then calculated for a single daily cycle, and under sunlight conditions covering the four seasons by selecting dates close to equinoxes and solstices of year 2010, i.e. 20th March, 21st June, 23rd September, and 23rd December of 2010. Note also that the Perez model (see section 5.1) has been parameterized in order to generate perfectly clear cloudless skies.

5.2.2 Canyon ~~modelling~~ modeling in TEB

5 In the same way, ~~the TEB model~~ TEB is run for equivalent configurations ~~but not exactly the same, since to SOLENE configurations, respecting~~ hypotheses, approaches, and spatial resolutions ~~are not identical in both~~ differences between the two models. For TEB simulations, the geometrical parameters describing the urban canyon form, as well as the height of trees and trunks are quite-comparable to those of ~~SOLENE~~ SOLENE simulations. But the different spatial arrangements of trees simulated by ~~SOLENE~~ SOLENE are simply prescribed as cover fractions in TEB. As a result, some configurations (~~for instance,~~ 10 e.g. B1 and B2 with different horizontal locations or B3 and B4 with different number of tree lines, shown in Fig.3) cannot be distinguished by the TEB approach, and are associated to the same cumulative cover fraction of tree canopy in TEB. In this manner, interactions between tree lines are not taken into account in TEB, contrary to SOLENE where rays are attenuated at each time crossing a mesh belonging to a vegetated envelope. All geometric features of both sets of simulations with ~~SOLENE~~ SOLENE and TEB are summarized in Table 2. In ~~SOLENE, the incident radiation flux is roughly attenuated of 50 % at once~~ when crossing a mesh of a vegetation envelope. In terms of process ~~modelling~~ modeling, the formulation of transmissivity of radiation through the foliage ~~according to a Beer Lambert law (Eq. 3) applied~~ in TEB is here simplified for the evaluation stage. In order to be consistent with the ~~SOLENE approach which applies an attenuation of 50 when radiation crosses a cell of the external envelope which composes the foliage, the downward exponential attenuation~~ SOLENE approach, the exponential attenuation expressing a maximum interception (including the Leaf Area Index) in Eq. 3, 4, 5 is replaced by ~~the expression~~ 20 $1 - 0.5(LAD/LAI)$ (see Appendix B for LAD details) 0.5 . The same way, the formulation proposed in Appendix B (Eq. B1, B2, B3, B4) for modulating the radiation attenuation depending on the likely path of rays and based on the Leaf Area Density profile, is here substituted by the expression $1 - 0.5(LAD/LAI)$, so that the maximum attenuation is 0.5 when all thickness of tree canopy is passed through. Note also that ~~the TEB model~~ TEB is forced by the same conditions of incoming solar radiation than those calculated for ~~SOLENE, in order to minimize gaps and differences in the two modelling approaches, that would~~ 25 ~~compromise the comparison of results.~~ the roofs in SOLENE. Using a unique forcing for each component (direct or diffuse) of the solar radiation from the SOLENE simulations, TEB forcings do not take into account the non-uniform distribution of incoming diffuse solar radiation. From this imprecision result differences from 1 to 4 % between the fluxes of the two walls, depending on their orientation, for studied aspect ratios during summertime (sensitive analysis not shown).

5.2.3 Comparison method

30 Finally, 880 solar radiation simulations are performed with both TEB and ~~SOLENE~~SOLENE models. For each of them, hourly outputs are stored. They include the direct and diffuse solar radiation received by the separated elements (*road, walls, and tree*) before multiple reflections, as well as the total ~~(direct and diffuse) solar radiation absorbed by the separated elements after multiple reflections~~shortwave radiation absorbed by the separate elements after multiple reflections. The main objective of the comparative exercise is to evaluate the cover fraction approach of TEB against a model (SOLENE) resolving the urban radiation budget at fine scale and with trees explicitly represented by geometrical elements. For this purpose, gaps between the simulations of received direct or diffuse solar radiation fluxes by canyon surfaces have been investigated. Because of divergent physics assumptions, the statistics concerning the absorption by the facets of the canyon need a cautious interpretation. During

5 multiple reflections, the radiation is assumed to be isotropic in TEB while SOLENE computes reflections with specular behavior using the method of radiosity. For comparing ~~SOLENE~~SOLENE and TEB, only the central part of the ~~SOLENE~~SOLENE's mock-up is used in order to avoid any boundary ~~effect~~effects (see the scheme in Fig. 3). For each flux, the values calculated by ~~SOLENE~~SOLENE are summed over all grid points that compose each element of the canyon (separately, the road, the two walls, and the trees). Finally, for both models~~SOLENE and TEB~~, the fluxes are weighted to be expressed according to the total

10 ground-based surface of the canyon, so that they can be compared to each other and compared to the incoming radiation. Note that tables with statistical scores presented hereafter have been fulfilled with the same procedure, i.e., the ~~root mean squared error~~(RMSE Mean Absolute Error (MAE in W m^{-2}), the ~~relative error~~(Err Mean Absolute Percentage Error (MAPE in %)) computed from the mean daily fluxes, and the mean bias (Bias in W m^{-2}), according to following equations: ~~RMSE=~~
(

The indexes i, j, k, l refer to as season, street orientation, aspect ratio of the street, and hour of the day, respectively, with

15 $n_s = 4, n_o = 4, n_h = 3, n_t = 24$. We also run simulations of the $h/w = 2$ additional cases where canyons are greened by a rescaled vegetation (see section 5.2.1 and Fig. 2).

6 Results

6.1 General analysis and seasonal effects

~~The table~~ Table 3 presents the statistical scores computed for the shortwave radiation absorbed by the different elements of the canyon, ~~for both cases, with and without vegetation. Note that the results are~~ Since multiple reflections are treated differently between TEB and SOLENE, these results are used to show the magnitude of variability of errors related to the presence of vegetation in the canyon or the considered season. Results are presented here by gathering the experiments performed with different street orientations and different vegetation layouts, but by distinguishing the seasons. In the light of the mean biases,

the TEB model tends to systematically overestimate the absorption by road and walls compared to ~~SOLENE~~-~~SOLENE~~ (up to ~~+5 and -9~~ ~~+16 and +10~~ $W m^{-2}$ for road and walls, respectively), and to underestimate the absorption by trees (up to ~~+8~~ ~~-19~~ $W m^{-2}$ ~~at maximum~~), whether the configuration or the season. ~~Let's remind that~~ ~~Considering that the~~ temperate climate is characterized by four ~~successive seasons with contrasted~~ ~~distinct seasons with contrasting~~ sunshine, air temperature and humidity conditions, ~~seasonal analysis was undertaken~~. Analysis of the results for each season separately indicates that relative errors (~~MAPE~~) are especially high for wintertime simulations for road and trees, due to a very low incoming solar radiation at that period. Nonetheless, the associated ~~RMSE and bias are quite acceptable (<10 and <~~ ~~MAE and biases are acceptable~~ (~~less than 3.5 and ± 3~~ $W m^{-2}$, respectively). Summer is the season which ~~gives~~ ~~provides~~ the best results ~~in terms of MAPE~~ when the canyon is tree-filled (~~relative errors~~ less than 25 %) or not (~~relative errors around~~ 3 %). This season is also the most relevant to be examined here because our first concern is to improve the simulation of the potential cooling effect of street trees in a urban environment, submitted to a strong ~~UHI~~ ~~Urban Heat Island~~ at this period. The evaluation is focused on effects of deciduous trees which are typical and widely present in cities under temperate climate. Such trees are leafless during winter, so that they have a negligible impact on thermal comfort and energy demand ~~at this season~~. That is why we focus on the summertime example hereafter, to assess the TEB performances for simulating the solar radiative exchanges in idealized canyons, vegetated or not.

6.2 Case of urban canyons without vegetation

The ~~TEB model's radiative calculations~~ ~~radiative calculations in TEB~~ are first evaluated for the cases without vegetation. Several comparisons with observations of radiation fluxes at ~~neighbourhood scale~~ ~~neighborhood scale~~ have been performed (~~Masson et al. (2002); Lemonsu et al. (2004, 2010); Pigeon et al. (2008)~~) (~~Masson et al., 2002; Lemonsu et al., 2004, 2010; Pigeon et al.,~~ They have shown a good capacity of the model in computing the upward short- and ~~long-wave~~ ~~long-wave~~ radiation at the top of the urban canopy, in real case configurations. But these evaluation exercises have not allowed us to ~~analyse~~ ~~analyze~~ separately the radiative contributions of various elements that compose the urban environment. Such a model-model comparison in a controlled framework is ideal to deeply investigate and evaluate the TEB radiation parameterizations.

Both direct and diffuse solar radiation received by the road and the separate walls before any ~~reflection~~ ~~reflections~~, as well as the total ~~solar~~ ~~shortwave~~ radiation absorbed by these surfaces, are studied. An example of daily cycle is presented in Fig. 4 for the case $h/w = 1$ and the four street orientations, for summer season. The scatterplots integrate all the hourly fluxes simulated for the three aspects ratios, the four street orientations, and the four seasons (Fig. 5). As expected, they demonstrate a strong positive linear relationship between fluxes calculated by ~~SOLENE and TEB models~~ ~~SOLENE and TEB~~ ($R^2 \geq 0.99$ except for diffuse solar radiation ~~absorbed~~ ~~absorbed~~ by roads: $R^2 = 0.979$).

The comparison between ~~SOLENE~~-~~SOLENE~~ and TEB simulations for the direct solar radiation received by road and walls before any ~~reflection~~ ~~reflections~~ highlights very good results. ~~The TEB model~~ ~~TEB~~ is able to reproduce the geometrical effects of the canyon on radiation penetration according to the time of the day, as well as the street orientation. For NE-SW and NW-

30 SE oriented streets, TEB simulates correctly the dissymmetry of fluxes between the two walls, as well as the temporal shift in peak of radiation received by the road in comparison with the N-S oriented street. For the E-W street case, the direct radiation received by the road is marked by a plateau effect between 8 am and 7 pm. The two walls have different ~~behaviours~~behaviors: the wall the most exposed to sun receives the maximum direct radiation at solar noon, whereas the most shaded wall receives direct radiation only early in the morning and late in the afternoon. The scores confirm the good performances of TEB: ~~RMSE is 8.91 and 4.54~~MAE are 4.39 and 2.49 W m^{-2} , and ~~bias is~~biases are -0.28 and +0.40 W m^{-2} for road and walls, respectively
35 ~~is 8.91 and 4.54~~MAE are 4.39 and 2.49 W m^{-2} , and ~~bias is~~biases are -0.28 and +0.40 W m^{-2} for road and walls, respectively (Table 4). They are associated with low ~~relative errors~~MAPE of only 1 % for both road and walls.

For the diffuse solar radiation calculations, ~~let's~~ remind that TEB does not separate the two walls. Consequently, here are compared in Fig. 4 the diffuse solar radiation flux received by the composite wall of TEB, and the average of the diffuse solar
5 radiation fluxes received by the separate walls of the ~~SOLENE~~SOLENE simulation. By considering an average surface, TEB underestimates the diffuse solar radiation received by walls in the morning and the afternoon, and it overestimates it at solar noon. ~~Inversely~~On the opposite, it overestimates the diffuse solar radiation received by the road in the morning and the afternoon, and it underestimates it at solar noon. In this case, ~~RMSE~~MAE and biases remain weak (~~<6 and <~~less than 3.5 and ± 1 W m^{-2} , respectively) because the involved fluxes are not very high (depending on the season, the diffuse component is
10 only 15-25 % of the total incident solar radiation), but ~~relative errors~~MAPE are slightly higher than for direct solar radiation, reaching 7 and 5 % for road and walls, respectively (Table 5). However, these discrepancies have no impact on performances of TEB neither at daily scale on fluxes of walls nor on instantaneous sum of cumulated canyon fluxes. Moreover, the dissymmetry of received diffuse solar radiation fluxes is no longer observed in ~~E/W oriented cases, where models are fitting very well for roads with relative errors less than 1~~E-W oriented cases.

15 Finally, the total ~~solar~~shortwave radiation absorbed by road and walls is well estimated by TEB despite the simplified hypotheses of the model and the use of a unique sky view factor by surface: ~~RMSE~~MAE and biases are ~~9.88~~6.03 and +3.50 W m^{-2} for road, respectively, and ~~5.72~~3.38 and +2.80 W m^{-2} for walls (Table 6). In view of the important incident radiation flux, exceeding 1 000 W m^{-2} at solar noon, the ~~relative error~~MAPE of 3 % for both surfaces remains moderate.

20 6.3 Case of urban canyons with vegetation

The same evaluations are conducted for vegetated canyons. The statistical scores are computed as previously (see Eq. ??, ??, ??) but by accounting for the 13 vegetation layouts. We also computed additional cases of vegetation layouts for the configurations referred to as "h/w = 2 rescaled vegetation" (see section 5.2.1. and Fig. 2 for further explanations). As an example, a comparison of hourly fluxes is presented in Fig. 6, for the layout A and an aspect ratio $h/w = 1$, and for the summer
25 daily cycle. This configuration is one of the most simple and comparable layouts between the two models: trees are 7.5 m high (i.e. almost the same height as buildings), tree crowns have a 5 m thickness, they are centered in the middle of the canyon and cover 90 % of the canyon width on the horizontal plane.

The daily evolution of direct solar radiation received by the different elements of the canyon can be compared to the case without vegetation (Fig. 4). The same patterns are obtained, whether for walls or road and the four street orientations, with an attenuation due to the presence of trees. Here, a significant part of direct incoming solar radiation is intercepted by the foliage. Due to its ~~semi-transparency properties (the transmissivity is here prescribed to 0.5)~~ partial transparency properties, the foliage allows at least half of radiation fluxes to pass through ~~-(see section 5.2.2.)~~. As a result, the urban surfaces (walls and road) receive less incoming direct radiation but are never totally obstructed by trees. These processes are correctly simulated by TEB ~~and the scores (based on the simulations at summertime) for the configuration A are quite acceptable: RMSE are 18.32, 6.86 and 10.04 W m⁻² for road, walls, and trees, respectively, with mean errors of 14, 5, and 4 only (Table 4).~~ Due with some limitations: due to the expression of direct solar radiation intercepted by high vegetation at the top of the crown which is treated as an horizontal surface in TEB ~~model~~ (Eq. 1), the fluxes reaching the trees in TEB are globally underestimated compared to the ~~SOLENE-SOLENE~~ fluxes that include contributions on the vertical faces of the crown envelope (Fig. 7 a., all seasons and configurations). Consequently, the solar radiation which is not intercepted by the tree layer in TEB simulations is assigned to the road ~~and the bottom of walls. This leads for configuration A to MAE of 9.18, 3.52 and 6.22 W m⁻² for road, walls, and trees, respectively, and MAPE of 14, 5, and 4 % only (Table 4).~~ The thicker the crown is, the greater is the error ~~(B1 vs associated to the tree (D1 vs B1 or B2 vs D2 vs B2), particularly when the tree rows are away from the walls (B1 vs B2, D1 vs D2 or D3 vs D4) and separated (B4 vs B3),~~ contrary to a continuous tree layer occupying almost the entire width of the canyon (A, C1, C2).

As expressed in Eq. 8 and 9, the diffuse solar radiation fluxes received by road and walls (walls are managed together as ~~a mean an average~~ surface), depends on the ~~sky-view sky view~~ factor of the given surface and on an attenuation coefficient of the incoming radiation through the foliage. Regarding all seasons ~~and configurations confounded~~, the received solar radiation by ground-based surfaces is also overestimated while the diffuse solar radiation flux reaching tree crowns is underestimated in the TEB simulations (Fig. 7 b.). Remind that the diffuse solar radiation received by the trees is calculated in TEB as the residual part of the incoming diffuse solar radiation flux which was not received by road and walls (see Eq. 10). Contrasted results are obtained for the vertical surfaces whether the vegetation layouts, in particular between double-row or centered trees (B3 vs B4). As previously discussed in section 5.4, these defects are related to the use of a single ~~sky-view sky view~~ factor for each surface, which is computed at mid-height of buildings for walls and in the middle of the street for road. ~~Since the~~ In addition, the isotropic nature of the diffuse solar radiation ~~received by the trees is calculated by TEB as the residual part of the incoming diffuse solar radiation which was not received by walls and road (see Eq. 10), it is inversely slightly underestimated leads to an exacerbation of the underestimation of the received flux by the high vegetation, particularly in cases where the side surface of vegetation envelopes is larger: for example, thick crowns with longer sides and vegetation layouts including two rows (the number of sides is doubled).~~ Considering the extremely vegetated canyon A, ~~relative errors MAPE~~ are 15, 9 and 20 % for road, walls, and tree, respectively, corresponding to ~~RMSE of 2.92, 2.72 and 5.42 MAE of 1.89, 1.51 and 3.51 W m⁻² (Table 5).~~ Globally, the estimation of the direct solar radiation received by the road and walls are acceptable regarding the MAPE which are $\leq 30\%$. However, the relative errors associated to the tree layer are contrasted (from 12 % to 49 %), depending on the

30 characteristics of the vegetation layout.

For ~~this configuration, the total solar~~ the same configuration, comparing TEB results to the SOLENE simulations as reference,
the total shortwave radiation absorbed by the different elements of the canyon is simulated with ~~a correct~~ a correct daily dynamics ~~and~~
~~good magnitudes~~, so that statistical scores are good: 27, 19 (Fig. 6). ~~Despite similar temporal behavior of the fluxes, their~~
magnitudes can greatly diverge, especially for the road and ~~5 of relative error for road, walls and tree~~, respectively, which
~~mean RMSE of only 19.67, 20.15 and 14.53~~ tree surfaces with MAPE greater than 30 % and biases greater than ± 25 W
 m^{-2} (Table 6). The global scatterplot (Fig. 7 c., all seasons and configurations) confirms ~~a good agreement between TEB and~~
~~SOLENE simulations ($R^2 \geq 0.90$) but an underestimation trend for the fluxes received and absorbed by trees is highlighted in~~
5 ~~some configurations.~~

6.4 Sensitivity to vegetation layout characteristics

The simple representation of tree canopy inside the canyon in the TEB model obviously present some limitations and can lead
to more or less important biases in the radiative calculations. On the basis of the diverse vegetation layouts that have been tested,
three issues are addressed here: (1) the effect of the tree horizontal coverage; (2) the effect of tree canopy height compared to
10 building height; and (3) the effect of tree location – centered or on side – in the canyon. The comparison of statistical scores for
the different vegetation layouts shows that the foliage horizontal coverage influences the performances of the TEB model (Fig.
8). In its parameterization of radiative exchanges, TEB represents the tree canopy as a layer of leaves which covers the total width
of the canyon but which is more or less diluted depending on the prescribed cover fraction (δ_t). This approach leads to better
results when this fraction is high (here for $\delta_t = 90\%$). The vertical location of tree canopy in relation to building height has
15 also a significant impact on TEB performances (Fig. 9). Both for direct and diffuse solar radiation received by road, walls, and
trees, the model gives better results when the foliage layer covers the high half of the canyon. The results are less good when
the foliage thickness is smaller, especially when the foliage layer is located in the middle part of the canyon. It is more difficult
to conclude on the influence of horizontal location. The differences seem less significant when comparing the configurations
for which the vegetation is centered along the canyon axis or located on the edge of the canyon (Fig. ??). By contrast, in case
20 of double lines of trees, it is noted that TEB simulates less well the direct and diffuse solar radiation received by road.

6.4 Analysis of an integrated mean daily canyon albedo

The mean daily albedo of the canyon (α_{can}) is calculated as the ratio between the outgoing shortwave radiation (which is
deduced from the difference between the incoming radiation $S_{can}^{\downarrow} + S_{can}^{\downarrow}$ and the absorbed radiation S_{can}^{*}) and the incoming
shortwave radiation:-

$$\frac{(S_{can}^{\downarrow} + S_{can}^{\downarrow})}{($$

For each simulation, these fluxes are integrated over the daily cycle in order to compute a mean canyon albedo for each case. The results are presented as boxplots (Fig. ??) that gather seasons, street orientations, vegetation layouts, but that distinguish the canyon aspect ratios. It is a synthetic indicator of TEB performance to estimate the shortwave radiative budget of trends previously found and the absorbed flux by the trees is underestimated. The predictability based on SOLENE results is also weaker ($R^2 = 0.945$). These poor performances of TEB regarding the statistical scores have to be interpreted with caution. This work aims at evaluating the cost in term of performances of TEB to simulate a correct allocation of radiative fluxes for each facet of the entire canyon, which is crucial when SURFEX is run coupled with an atmospheric model such as the research model MESO-NH (Lafore et al., 1997) or the numerical prediction model AROME (Seity et al., 2011). The previous comparisons (section 6.2) have shown that TEB tends to slightly overestimate the solar absorption by road and walls in case of non-vegetated canyons, so that the mean canyon albedo is slightly weaker than in SOLENE: -1.5 for canyon in spite of a simple approach based on cover fraction. For example, the tree fraction is computed as a cumulative fraction of all crowns in the street in TEB. Thus, the -2.5 interactions between tree lines are not allowed, contrary to in SOLENE. However, some physical differences limit the comparison of the absorbed fluxes. Indeed, the way to calculate the multiple reflections is dissimilar between the two models (see section 5.2.3). TEB code computes infinite isotropic reflections using a unique view factor for each facet of the canyon and mean radiative transmissivity terms. Remind that the mean radiative transmissivity terms are based on strong hypotheses on the path of rays considering the studied interaction (see Appendix B). On the contrary, SOLENE radiative scheme computes multiple reflections as specular radiation within the canyon for $-$ and -3.5 for $-$. This underestimation is less marked for wide canyons because sunlight can totally penetrate and enlighten walls or ground-based surfaces; in this configuration, the approximation related to the use of unique sky-view-factor per surface is less disadvantageous than in case of narrow canyons. For vegetated canyons, the tree canopy absorbs less solar radiation in TEB than in SOLENE whereas the absorption by road and walls remains underestimated. Despite the combination of these compensatory effects, the mean canyon albedo is systematically underestimated by TEB, which translates a global overestimation of solar radiation absorption by the canyon. This defect is accentuated for narrow canyons. In case of or 1 the mean error for (α_{can}) is less than 10 and 22, respectively, but exceeds 35 for greater aspect ratios. In case of vegetated canyons, two simplifications may explain these biases: the use of a unique sky-view-factor for each surface, and each triangular mesh and using the radiosity method. The vegetation envelopes are strictly semi-transparent because the calculation of the sky-view-factor for high vegetation which is done at the mid-height of the crown, penetration of light through the foliage can not be modulated by the Leaf Area Density. Whatever the foliage thickness which is crossed, as soon as a ray reaches a cell of vegetation envelope in SOLENE, this radiation is attenuated by half.

Finally, one can note the variability of (α_{can}) obtained with TEB is less than with SOLENE (Fig. ??) since TEB cannot manage differently some horizontal arrangements of the vegetation layouts (e.g. B1 and B2 configurations, see Fig. 3) Further works (not shown) have investigated the sensitivity of TEB results and performances according to the characteristics of the different vegetation layouts. They do not demonstrate clear and systematic patterns when studying the impact of: (1) tree horizontal coverage (or the tree fraction); (2) tree canopy height compared to the building height; (3) tree location - centered or on side

30 - in the canyon on the MAE and error percentages recorded. It could be explained by the interaction between opposite effects regarding the vegetation layouts characteristics.

6.4 ~~Benefit~~ Benefits of TEB developments

6.4.1 Analysis of the mean daily absorbed shortwave radiation by the canyon

The shortwave radiation received and absorbed by the walls and the road can be strongly affected by the presence of tree vegetation. The comparison between the initial version of TEB which deals with vegetation at ground level, and the new version which explicitly includes an additional tree stratum, shows differences (Fig. ??). ~~The solar~~. Before weighting the fluxes by the appropriate cover fractions, the shortwave radiation absorbed by the urban facets (road and vertical surfaces) is ground-based surfaces are largely overestimated in the TEB initial version, since the shadowing effects by tree vegetation are not taken into account. Inversely, the vegetation is much more subject to shade of buildings since it is assumed to be on the ground for radiative calculations. With the configuration A as an example (i. e., with a tree coverage of 90 initial version of TEB (+ 77% inside the canyon, see Fig. 3), the reference version of the TEB model is characterized by an overestimation in solar for road and +66% for the garden in the case A in summer). These defects highlight the lack of representation of the interception of rays before reaching the road related to a reduced absorption of the vegetation by its transparency properties. On the opposite, we observe an underestimation of the absorbed flux regarding the two walls: -41% for wall A and -53% for wall B. It is explained because during multiple reflections, the tree layer (which is thick in case A) facing walls accentuates the absorption of vertical surfaces in the implemented version. Nonetheless, weighting the fluxes at the canyon scale affects greatly the road and garden fractions. In the reference cases, the high vegetation is treated as a ground-based vegetation fraction which is included in the garden fraction (δ_g). Consequently, the road fraction, which is always defined as $1 - \delta_g$, is varying according to the vegetation layout. In this way, compared to the current version, a larger absorbed shortwave radiation flux in W m^{-2} of road may lead to a lower flux expressed in W m^{-2} of canyon when the garden fraction is high. During the summer and all configurations confounded (Fig. 8), we observe a mean underestimation of the shortwave radiation absorption of +80 -44% for the road and +64 -10% for the walls, while an underestimation of -6 is noted for the trees, compared to the implemented TEB-version. This can have a significant impact on thermal comfort conditions for pedestrians as well as on energy consumption of buildings for air-conditioning usage.

However Moreover, the reference case presents a strong dispersion in the simulation of solar fluxes absorbed by roadthe vegetation, depending on the configurations (aspect ratio of canyon, street orientation, and season and vegetation layout). In some cases especially, the solar flux absorbed by vegetation this flux is greater than in the new version of TEB. This effect is related to the fact that the reference version does not treat the vegetation as a semi-transparent object and does not take into account its transmissivity properties. As a result, the vegetation absorbs all the solar radiation which is received and not reflected. In the present case, this part is 75 % of the incident solar radiation since $\alpha_t = 0.25$. In the new version, 50 % of the received solar radiation is transmitted through the foliage and 75 % of the remaining flux is absorbed by trees, i.e. 37.5

30 % of the total solar-shortwave radiation received by trees. On the other hand, this defect could be counterbalanced by the fact that vegetation is much more submitted to shade of buildings since it is assumed to be on the ground in the former version of radiative calculations. The mean underestimation of the initial version is -6% but the boxplots show opposite tendencies regarding the medians because of contrasted results among the latest simulations.

6.4.2 Analysis of an integrated mean daily canyon albedo

5 The mean daily albedo of the canyon (α_{can}) is calculated as the ratio between the outgoing shortwave radiation (which is deduced from the difference between the incoming radiation $S_{can}^{\downarrow} + S_{can}^{\downarrow}$ and the absorbed radiation S_{can}^*) and the incoming shortwave radiation:

$$(S_{can}^{\downarrow} + S_{can}^{\downarrow})$$

(20)

10

For each simulation, these fluxes are integrated over the daily cycle in order to compute a mean canyon albedo for each case. The results in summertime are presented as boxplots (Fig. 9) that gather street orientations, vegetation layouts, but that distinguish the canyon aspect ratios. It is a synthetic indicator of TEB enhancement at the scale of the entire canyon, which is crucial when SURFEX is run coupled with an atmospheric model such as the research MESO-NH model (Lafore et al., 1997) or the operational model named AROME (Seity et al., 2011) to provide climatic simulations.

20 Since the geometry and radiative properties of the vegetationless canyons and ground-based vegetation canyons in the reference version of TEB are comparable, they provide similar canyon albedos. It is explained by the absence of foliage in the vertical plane and identical albedos of road and garden ($\alpha_r = \alpha_g = 0.25$). Their canyon albedos rise with an increasing aspect ratio. This demonstrates the impact of greater shading effects of walls on the total absorption by the facets in deep streets, restraining the penetration of the light. No differences are observed between simulations of $h/w = 2$ canyons since the ground-based vegetation have no defined thickness. On the opposite, the canyon albedo of the implemented version of TEB strongly decreases with an increasing aspect ratio. It is expected results because the absorption is enhanced by correcting the height of the intercepting surface at the first reflection (Eq. 1) which is less shaded by the buildings than a ground-based surface. Moreover, the trapping effect is strengthened by the presence of the canopy within the canyon during the multiple reflections. Adding the processes of attenuation occurring at each interactions between the other facets or the sky (Eq. B1, B2, B3, B4) also contributes to improve the simulation of albedo by the current TEB version. We observe a greater variability of the mean daily canyon albedo after the implementation of an explicit high vegetation stratum for the $h/w = 1$ urban forms for which the

25

30 weight of the tree fraction is relatively higher. In deep streets, the impact of the vegetation layout on the canyon albedo depends on the location of the trees. When the canopy fills the low part of a $h/w = 2$ canyon, vegetation have a limited influence, contrary to cases with rescaled vegetation in comparable urban forms.

7 Conclusions

In order to investigate some of the physical processes related to the presence of vegetation in urban environment, e.g. for microclimate, hydrology or building energy consumption issues, the modeling is definitely a necessary tool.

The TEB model has been refined and improved in order to explicitly represent street trees and their impacts on radiative transfers. The new parameterization is based on the quite-simple hypotheses of TEB: (1) a little detailed geometry without specific spatial arrangement of ground-based surfaces and (2) a single view factor to each emitting and receiving surface applied for radiative calculations.

To take into account the tree canopy in TEB, it was however required to add a new vegetated stratum on the vertical plane, which can ~~superimpose to road and shade the road, the walls and the~~ low vegetation. This modification ~~has obviously complexified the led to more complex~~ radiative calculations, but has been done with a concern to preserve a certain level of simplicity and to limit the number of new input parameters for TEB. It is important to emphasize that the model is designed to be run over whole cities, for which it can simulate the local climatic variability related to urban landscape heterogeneities at the neighborhood scale. This means that computing times must be acceptable, and that input urban data must be available or quite-easy to define. Consequently, the high vegetation is here described using only five input parameters: cover fraction of trees, height of trees, height of trunks, ~~LAI, Leaf Area Index~~ and albedo.

This simplified characterization of high vegetation necessarily induces some uncertainties on solar radiative exchanges. ~~This has been highlighted here through the comparison of TEB with~~ We estimated it by carrying out a comparative exercise between TEB and a high spatial-resolution solar and lighting model (SOLENE). ~~The TEB results are nonetheless quite acceptable for the majority of studied configurations in terms of canyon geometry, street orientation, vegetation layout, or sunshine conditions. Indeed, TEB simulations of SOLENE).~~ On the basis of an idealized geometry of urban canyon with various vegetation layouts, TEB is evaluated regarding the direct and diffuse solar radiation received by the elements that compose the canyon. TEB simulations in summer gathered best scores ($|bias| < 20 \text{ W m}^{-2}$) for all configurations and surfaces considered, which is precisely the most relevant season to assess the cooling effect of deciduous trees under temperate climate. Statistical scores have demonstrated a good capacity of TEB to solve the radiative balance of canyons without vegetation despite the use of a unique sky view factor for each facet of the urban scene. Biases less than $\pm 1 \text{ W m}^{-2}$ related to the direct and diffuse solar radiation fluxes received by road and vertical surfaces have been recorded. Additionally, it is necessary to put in perspective obtained scores with the fact that they include the error generated by the treatment of walls as a mean wall in TEB in com-

30 parison with separate walls of ~~SOLENE~~SOLENE. This identified error is no longer existing at the canyon or daily scales. ~~The study of mean daily canyon albedos reveals mean errors less than 9 for and 22 for~~ Concerning the vegetated canyons we noted a high variability of statistical scores depending on the vegetation layout. The greater uncertainties are found for the solar radiation fluxes received by the high vegetation. The Mean Absolute Error averaged over the vegetation configurations during summertime is $17.27 \pm 9.31 \text{ W m}^{-2}$ for the direct component and $3.45 \pm 1.93 \text{ W m}^{-2}$ for the diffuse component but these
35 scores are associated to acceptable biases: $-14.44 \pm 10.60 \text{ W m}^{-2}$ and $-3.21 \pm 2.20 \text{ W m}^{-2}$, respectively. ~~Despite of worse results for higher aspect ratios, the vegetalization of very large avenues with medium or high buildings is more likely than within narrower and deeper streets~~The systematic underestimation of fluxes reaching the new tree stratum is explained by the cover fraction approach in TEB where sides of the crown are not represented.

5 The parameterization of shortwave radiation exchanges within the canyon is now more realistic: shading effects of trees on vertical and ground-based surfaces but also shading effects of buildings on trees are computed. This is achieved by adding a new specific cover fraction describing the horizontal extend of high vegetation. Infinite reflections within the canyon are also conditioned to the transmissivity term calculated per pairs of exchanging surfaces. This study demonstrate the enhancement of new developments on the computed absorbed shortwave radiation fluxes within the canyon between the former reference version of TEB and the implemented version. In the current version, trees can intercept and absorb the direct solar radiation at the canopy level instead of from the ground. Consequently, the walls are more shaded. The road fraction is now independent of the cover of high vegetation. This implies that the weighting of fluxes at the canyon scale is correct. The mean daily canyon albedo is lesser than in reference cases in relation with a better representation of the radiation trapping. Canyon albedo is also more vegetation-responsive for $h/w = 1$ urban forms or in cases with $h/w = 2$ canyons when the vegetation is scaled regarding the depth of the street.

5 The future developments will focus on the separate calculation of turbulent energy fluxes for ground-based and high vegetation. The aerodynamic effect of trees on air flow within the canyon should also be parameterized. Based on this more sophisticated version of ~~the TEB model~~TEB, new impact studies could be conducted and greening adaptation strategies could be evaluated more precisely.

10 8 Code availability

The TEB code is available in open source via the surface ~~modelling~~modeling platform called SURFEX, downloadable at <http://www.cnrm-game-meteo.fr/surfex/>. This Open-SURFEX will be updated at relatively low frequency (each 3 to 6 months) and developments presented here are not included in the last version yet. If you need more frequent updates, or if you need what is not in Open-SURFEX (DrHOOK, FA/LFI formats, GAUSSIAN grid), we invite you to follow the procedure to get a
15 SVN account and to access real-time modifications of the code (see instructions at the previous link).

Appendix A: ~~Sky-view~~Sky view and view factors

~~Sky-view-factors~~Sky view factors for road, garden and wall (Eq. ~~??~~A1, A2) as well as the view factors between elements remain unchanged in relation to initial version of the radiative calculations in TEB (described in Masson (2000) and Lemonsu et al. (2012)):

$$20 \quad \Psi_{rs} = \Psi_{sr} = \sqrt{\left(\frac{h}{w}\right)^2 + 1} - \frac{h}{w} \quad (\text{A1})$$

$$\Psi_{wr} = \Psi_{ws} = \frac{\frac{1}{2} \left(\frac{h}{w} + 1 - \sqrt{\left(\frac{h}{w}\right)^2 + 1} \right)}{\frac{h}{w}} \quad (\text{A2})$$

$$\Psi_{sw} = 1 - \Psi_{sr} \quad (\text{A3})$$

$$25 \quad \Psi_{ww} = 1 - 2\Psi_{ws} = \frac{\sqrt{\left(\frac{h}{w}\right)^2 + 1} - 1}{\frac{h}{w}} \quad (\text{A4})$$

$$\Psi_{rw} = 1 - \Psi_{rs} = 1 - \left(\sqrt{\left(\frac{h}{w}\right)^2 + 1} - \frac{h}{w} \right) \quad (\text{A5})$$

For the tree canopy, the ~~sky-view-factor~~sky view-factor and view factors from road and walls are computed in the middle of the canyon and at mid-height of crown:

$$\Psi_{st} = \sqrt{\left(\frac{h}{w} \cdot \frac{h - h_{cw}}{h}\right)^2 + 1} - \left(\frac{h}{w} \cdot \frac{h - h_{cw}}{h}\right) \quad (\text{A6})$$

$$\Psi_{rt} = \sqrt{\left(\frac{h}{w} \cdot \frac{h_{cw}}{h}\right)^2 + 1} - \left(\frac{h}{w} \cdot \frac{h_{cw}}{h}\right) \quad (\text{A7})$$

$$10 \quad \Psi_{wt} = 1 - \frac{2}{2} \left(\Psi_{st} + \Psi_{rt} \right) \quad (\text{A8})$$

Appendix B: Mean radiative transmissivity of canyon tree canopy

The multiple reflections of solar radiation inside the canyon (as detailed in Masson (2000) and Lemonsu et al. (2012)) are now affected by the presence of trees whose foliage intercepts, reflects and absorbs a part of the energy. The transmissivity of

radiation through the foliage of tree canopy is variable according to the way the rays cross the foliage and the distance they travel. According to the location of tree crowns inside the canyon and the dominant orientation of radiation (e.g. emission from sky to ground or from wall to ground do not reach the foliage the same way), these rays can cross all the foliage thickness or only a small portion. The vertical distribution of leaves in the tree crowns has also an impact on transmissivity.

20

Different transmissivity functions (referred to as τ_{12} for exchanges between element 1 and element 2) are calculated depending of the surfaces involved in radiation-radiative exchanges. One distinguishes four cases of radiation exchanges, by hypothesizing that transmissivity functions are symmetric, i.e., exchanges from element 1 to element 2 is equivalent to the reverse way: between ground-based surfaces and sky ($\tau_{rs} = \tau_{sg}$) or wall ($\tau_{rw} = \tau_{gw}$), between wall and sky (τ_{ws}), between wall and wall

25 (τ_{ww}). For each case we admit, according to Lee and Park (2008), that majority of radiation exchanges occurs in a specific zone of the canyon, for which the Leaf Area Density (LAD_t expressed in ~~m^3 of leaves per m^2~~ of groundleaf area per m^3 of volume) is calculated:

$$\tau_{rs} = 1 - \delta_t \left[1 - \exp\left(-k \int_0^h LAD_t dz\right) \right] \quad (B1)$$

$$\tau_{rw} = 1 - \delta_t \left[1 - \exp\left(-k \int_0^{\frac{h}{2}} LAD_t dz\right) \right] \quad (B2)$$

$$\tau_{ws} = 1 - \delta_t \left[1 - \exp\left(-k \int_{\frac{h}{2}}^h LAD_t dz\right) \right] \quad (B3)$$

5

$$\tau_{ww} = 1 - \delta_t \left[1 - \exp\left(-k \int_{\frac{h}{4}}^{\frac{3h}{4}} LAD_t dz\right) \right] \quad (B4)$$

Note that this expression is these expressions are in accordance with the one applied in Eq. ??3 in which LAD_t is integrated on the complete-entire thickness of foliage so that it is equivalent to LAI_t . As mentioned above, since the tree crown is described as a parallelepiped with a regular distribution of leaves, a uniform vertical profile of LAD is here applied.

10 Appendix C: Total solar-shortwave radiation absorption by solving infinite reflections

For solar radiation calculations, the TEB model takes into account an infinite number of reflections between all elements composing the urban canyon. At each reflection, the isotropic radiation intercepted by a given element (1) after reflections on one of the other elements (2) is conditioned by the view factor of (2) from (1) referred to as Ψ_{12} (see Appendix A), the mean radiative transmissivity τ_{12} (see Appendix B) and the reflection is then determined according to reflective properties of (1). As

15 seen in the section 4.4, the total solar-shortwave radiation absorbed by each elements of the canyon or redirected towards the

sky is function of infinite reflections R_∞ , G_∞ , A_∞ , B_∞ , and T_∞ that are still unknowns at this stage. These terms **involve include** the first reflection on each element: R_0 , G_0 , A_0 , B_0 , T_0 . For road, garden, and walls, R_0 , G_0 , A_0 and B_0 simply depend on the incident solar radiation on the surface and the albedo. From the equations 14, 15, 16, 17 and 18, we can deduce the reflected part occurring at the $n + 1^{th}$ absorption as the complementary term of the $n + 1^{th}$ solar radiation reception for only 20 opaque elements of the canyon, *road*, *garden*, *wall A*, and *wall B*, respectively. As **an-exampleexamples**, we obtain for road **and wall A, respectively**:

$$R_0 = \alpha_r (S_r^\downarrow + S_r^\uparrow) \quad (C1)$$

$$R_{n+1} = R_0 + \alpha_r [\Psi_{rw}\tau_{rw}W_n + \underline{c_{rt}}\Psi_{rt}\delta_t T_n] \quad (C2)$$

25 $A_0 \equiv \underline{\alpha_w (S_w^\downarrow + S_w^\uparrow)} \quad (C3)$

$$\underline{A_{n+1}} \equiv \underline{A_0 + \alpha_w [\Psi_{ww}\tau_{ww}B_n + \Psi_{wr}\tau_{wr}(\delta_r R_n + \delta_g G_n) + c_{wt}\Psi_{wt}\delta_t T_n]} \quad (C4)$$

The specific coefficients associated to the view factors related to the high vegetation in shortwave reflections calculations are defined as:

$$\underline{c_{rt}} \equiv 0 \quad (C5)$$

$$\underline{c_{wt}} \equiv$$

5 $\underline{2 - \Psi_{st} - \Psi_{rt}}$ (C6) Only reflections from trees to sky or top part of walls are allowed. As explained in section 4.4, this mode of reflection by the leaves during the first reflection, which is by far the most energetic one, is more likely to occur than in an isotropic way. This assumption could be easily bypassed by fixing the previous coefficients to 1.

For the first tree canopy reflection, the part of received direct solar radiation is corrected by the transmitted flux (see Eq. 2):

$$T_0 = \alpha_t [(S_t^\downarrow - S_t^\uparrow) + S_t^\downarrow] \quad (C7)$$

10 Some uncertainties remain about relevance of **sky-view-sky view** or view factors which ones could formulate to represent reflective contributions from other surfaces at n^{th} to the absorption or reflection by the tree layer at $n + 1^{th}$, as well as potential absorption of energy within the tree's crown. Consequently, the solar flux reflected by *tree* at $n + 1^{th}$ has been determined as the residual term by assuming that the n^{th} solar reflection coming from each element (*road*, *garden*, *wall A*, and *wall B*) which is not received by *road*, *garden*, *wall A*, *wall B* or which is not returned to *sky* at $n + 1$ is received by *tree*.

15 During each interreflection, a part of n^{th} reflected flux which is potentially available for the $(n + 1)^{th}$ reflection or absorption is intercepted by high vegetation. This intercepted part related to the presence of foliage on the way of scattered rays towards each receiving element or sky are formulated as following:

$$I_s(n+1) = \Psi_{sr}(1-\tau_{sr})(\delta_r R_n + \delta_g G_n) + \Psi_{sw}(1-\tau_{sw}) \frac{A_n + B_n}{2} \quad (C8)$$

20

$$I_r(n+1) = \Psi_{rw}(1-\tau_{rw}) \frac{A_n + B_n}{2} \quad (C9)$$

$$I_g(n+1) = \Psi_{rw}(1-\tau_{rw}) \frac{A_n + B_n}{2} \quad (C10)$$

$$I_{w_A}(n+1) = \Psi_{wr}(1-\tau_{wr})(\delta_r R_n + \delta_g G_n) + \Psi_{ww}(1-\tau_{ww}) B_n \quad (C11)$$

$$I_{w_B}(n+1) = \Psi_{wr}(1-\tau_{wr})(\delta_r R_n + \delta_g G_n) + \Psi_{ww}(1-\tau_{ww}) A_n \quad (C12)$$

5 Finally, the solar flux which is intercepted by *tree* at $(n+1)$ is expressed as the sum of interceptions on the way of receiving elements of the canyon or sky:

$$I_t(n+1) = \frac{1}{\delta_t} \left(I_s(n+1) + \delta_r I_r(n+1) + \delta_g I_g(n+1) + \frac{2h}{w} \frac{I_{w_A}(n+1) + I_{w_B}(n+1)}{2} \right) \quad (C13)$$

The solar energy which is reflected by tree at $(n+1)$ is ~~consequently:~~ consequently:

$$T_{n+1} = \alpha_t I_t(n+1) \quad (C14)$$

10 ~~As a result, after an infinite number of reflections, the equation system can be written:-~~

$$\underline{R_\infty} \equiv \underline{R_0 + \alpha_r [\Psi_{rw} \tau_{rw} W_\infty + \Psi_{rt} \delta_t T_\infty]}$$

$$\underline{G_\infty} \equiv \underline{G_0 + \alpha_g [\Psi_{rw} \tau_{rw} W_\infty + \Psi_{rt} \delta_t T_\infty]}$$

$$\underline{W_\infty} \equiv \underline{W_0 + \alpha_w [\Psi_{ww} \tau_{ww} W_\infty + \Psi_{wr} \tau_{rw} (\delta_r R_\infty + \delta_g G_\infty) + \Psi_{wt} \delta_t T_\infty]}$$

$$\underline{T_\infty} \equiv \underline{T_0 + \frac{\alpha_t}{\delta_t} [(\Psi_{sw}(1-\tau_{sw}) + \Psi_{rw}(1-\tau_{rw}) + \Psi_{ww}(1-\tau_{ww})) W_\infty}$$

$$+ (\Psi_{sr}(1-\tau_{sr}) + \Psi_{wr}(1-\tau_{wr})) (\delta_r R_\infty + \delta_g G_\infty)]$$

15

The formulations can be simplified by gathering the equations for walls in a single expression for a mean wall according to:

$$W(n+1) = \frac{A(n+1) + B(n+1)}{2} \quad (C15)$$

As a result, after an infinite number of reflections, the equation system can be written:

$$\underline{R_\infty} \equiv \underline{R_0 + \alpha_r [\Psi_{rw} \tau_{rw} W_\infty + c_{rt} \Psi_{rt} \delta_t T_\infty]} \quad (\text{C16})$$

$$20 \quad \underline{G_\infty} \equiv \underline{G_0 + \alpha_g [\Psi_{rw} \tau_{rw} W_\infty + c_{rt} \Psi_{rt} \delta_t T_\infty]} \quad (\text{C17})$$

$$\underline{W_\infty} \equiv \underline{W_0 + \alpha_w [\Psi_{ww} \tau_{ww} W_\infty + \Psi_{wr} \tau_{rw} (\delta_r R_\infty + \delta_g G_\infty) + c_{wt} \Psi_{wt} \delta_t T_\infty]} \quad (\text{C18})$$

$$\underline{T_\infty} \equiv \underline{T_0 + \frac{\alpha_t}{\delta_t} [(\Psi_{sw}(1 - \tau_{sw}) + \Psi_{rw}(1 - \tau_{rw}) + \Psi_{ww}(1 - \tau_{ww})) W_\infty + (\Psi_{sr}(1 - \tau_{sr}) + \Psi_{wr}(1 - \tau_{wr})) (\delta_r R_\infty + \delta_g G_\infty)]} \quad (\text{C19})$$

As a result, we resolve the linear system of four equations with four unknowns:

$$R_\infty = R_0 + \mathcal{F}_{rw} W_\infty + \mathcal{F}_{rt} T_\infty \quad (\text{C20})$$

$$G_\infty = G_0 + \mathcal{F}_{gw} W_\infty + \mathcal{F}_{gt} T_\infty \quad (\text{C21})$$

$$W_\infty = W_0 + \mathcal{F}_{ww} W_\infty + \mathcal{F}_{wr} R_\infty + \mathcal{F}_{wg} G_\infty + \mathcal{F}_{wt} T_\infty \quad (\text{C22})$$

$$5 \quad T_\infty = T_0 + \mathcal{F}_{tw} W_\infty + \mathcal{F}_{tr} R_\infty + \mathcal{F}_{tg} G_\infty \quad (\text{C23})$$

The geometric and reflective factors are computed as following:

$$\mathcal{F}_{rw} = \Psi_{rw} \tau_{rw} \alpha_r \quad (\text{C24})$$

$$\mathcal{F}_{rt} = \underline{c_{rt}} \Psi_{rt} \delta_t \alpha_r \quad (\text{C25})$$

$$\mathcal{F}_{gw} = \Psi_{rw} \tau_{rw} \alpha_g \quad (\text{C26})$$

$$10 \quad \mathcal{F}_{gt} = \underline{c_{rt}} \Psi_{rt} \delta_t \alpha_g \quad (\text{C27})$$

$$\mathcal{F}_{wr} = \Psi_{wr} \tau_{wr} \delta_r \alpha_w \quad (\text{C28})$$

$$\mathcal{F}_{wg} = \Psi_{wr} \tau_{wr} \delta_g \alpha_w \quad (\text{C29})$$

$$\mathcal{F}_{ww} = \Psi_{ww} \tau_{ww} \alpha_w \quad (\text{C30})$$

$$\mathcal{F}_{wt} = \underline{0.5c_{wt}} \Psi_{wt} \delta_t \alpha_w \quad (\text{C31})$$

$$15 \quad \mathcal{F}_{tw} = [\Psi_{sw}(1 - \tau_{sw}) + \Psi_{rw}(1 - \tau_{rw}) + \Psi_{ww}(1 - \tau_{ww})] \frac{1}{\delta_t} \alpha_t \quad (\text{C32})$$

$$\mathcal{F}_{tr} = [\Psi_{sr}(1 - \tau_{sr}) + \Psi_{wr}(1 - \tau_{wr})] \frac{\delta_r}{\delta_t} \alpha_t \quad (\text{C33})$$

$$\mathcal{F}_{tg} = [\Psi_{sr}(1 - \tau_{sr}) + \Psi_{wr}(1 - \tau_{wr})] \frac{\delta_g}{\delta_t} \alpha_t \quad (\text{C34})$$

The resolution of the equation system gives the following expressions for multiple reflections on tree, walls, road, and garden:

$$\begin{aligned}
20 \quad T_\infty = & \left(\frac{1 - \mathcal{F}_{wr}\mathcal{F}_{rw} - \mathcal{F}_{wg}\mathcal{F}_{gw} - \mathcal{F}_{ww}}{\mathcal{D}} \right) T_0 \\
& + \left(\frac{\mathcal{F}_{tr}(1 - \mathcal{F}_{wg}\mathcal{F}_{gw} - \mathcal{F}_{ww}) + \mathcal{F}_{wr}(\mathcal{F}_{tg}\mathcal{F}_{gw} + \mathcal{F}_{tw})}{\mathcal{D}} \right) R_0 \\
& + \left(\frac{\mathcal{F}_{tg}(1 - \mathcal{F}_{wr}\mathcal{F}_{rw} - \mathcal{F}_{ww}) + \mathcal{F}_{wg}(\mathcal{F}_{tr}\mathcal{F}_{rw} + \mathcal{F}_{tw})}{\mathcal{D}} \right) G_0 \\
& + \left(\frac{\mathcal{F}_{tr}\mathcal{F}_{rw} + \mathcal{F}_{tg}\mathcal{F}_{gw} + \mathcal{F}_{tw}}{\mathcal{D}} \right) W_0
\end{aligned} \tag{C35}$$

$$\begin{aligned}
25 \quad W_\infty = & \left(\frac{\mathcal{F}_{wr}\mathcal{F}_{rt} + \mathcal{F}_{wg}\mathcal{F}_{gt} + \mathcal{F}_{wt}}{\mathcal{D}} \right) T_0 \\
& + \left(\frac{\mathcal{F}_{wr}(1 - \mathcal{F}_{tg}\mathcal{F}_{gt}) + \mathcal{F}_{tr}(\mathcal{F}_{wg}\mathcal{F}_{gt} + \mathcal{F}_{wt})}{\mathcal{D}} \right) R_0 \\
& + \left(\frac{\mathcal{F}_{wg}(1 - \mathcal{F}_{tr}\mathcal{F}_{rt}) + \mathcal{F}_{tg}(\mathcal{F}_{wr}\mathcal{F}_{rt} + \mathcal{F}_{wt})}{\mathcal{D}} \right) G_0 \\
& + \left(\frac{1 - \mathcal{F}_{rt}\mathcal{F}_{tr} - \mathcal{F}_{tg}\mathcal{F}_{gt}}{\mathcal{D}} \right) W_0
\end{aligned} \tag{C36}$$

$$\begin{aligned}
5 \quad R_\infty = & \left(\frac{\mathcal{F}_{rw}(\mathcal{F}_{rt}\mathcal{F}_{wr} + \mathcal{F}_{gt}\mathcal{F}_{wg} + \mathcal{F}_{wt}) + \mathcal{F}_{rt}(1 - \mathcal{F}_{wr}\mathcal{F}_{rw} - \mathcal{F}_{wg}\mathcal{F}_{gw} - \mathcal{F}_{ww})}{\mathcal{D}} \right) T_0 \\
& + \left(1 + \frac{\mathcal{F}_{rw}(\mathcal{F}_{wr}(1 - \mathcal{F}_{tg}\mathcal{F}_{gt}) + \mathcal{F}_{tr}(\mathcal{F}_{wg}\mathcal{F}_{gt} + \mathcal{F}_{wt})) + \mathcal{F}_{rt}(\mathcal{F}_{tr}(1 - \mathcal{F}_{wg}\mathcal{F}_{gw}) + \mathcal{F}_{wr}(\mathcal{F}_{tg}\mathcal{F}_{gw} + \mathcal{F}_{tw}))}{\mathcal{D}} \right) R_0 \\
& + \left(\frac{\mathcal{F}_{rw}(\mathcal{F}_{wg}(1 - \mathcal{F}_{tr}\mathcal{F}_{rt}) + \mathcal{F}_{tg}(\mathcal{F}_{wr}\mathcal{F}_{rt} + \mathcal{F}_{wt})) + \mathcal{F}_{rt}(\mathcal{F}_{tg}(1 - \mathcal{F}_{wr}\mathcal{F}_{rw} - \mathcal{F}_{ww}) + \mathcal{F}_{wg}(\mathcal{F}_{tr}\mathcal{F}_{rw} + \mathcal{F}_{tw}))}{\mathcal{D}} \right) G_0 \\
& + \left(\frac{\mathcal{F}_{rt}(\mathcal{F}_{tr}\mathcal{F}_{rw} + \mathcal{F}_{tg}\mathcal{F}_{gw} + \mathcal{F}_{tw}) + \mathcal{F}_{rw}(1 - \mathcal{F}_{tr}\mathcal{F}_{rt} - \mathcal{F}_{tg}\mathcal{F}_{gt})}{\mathcal{D}} \right) W_0
\end{aligned} \tag{C37}$$

$$\begin{aligned}
10 \quad G_\infty = & \left(\frac{\mathcal{F}_{gw}(\mathcal{F}_{rt}\mathcal{F}_{wr} + \mathcal{F}_{gt}\mathcal{F}_{wg} + \mathcal{F}_{wt}) + \mathcal{F}_{gt}(1 - \mathcal{F}_{wr}\mathcal{F}_{rw} - \mathcal{F}_{wg}\mathcal{F}_{gw} - \mathcal{F}_{ww})}{\mathcal{D}} \right) T_0 \\
& + \left(\frac{\mathcal{F}_{gw}(\mathcal{F}_{wr}(1 - \mathcal{F}_{tg}\mathcal{F}_{gt}) + \mathcal{F}_{tr}(\mathcal{F}_{wg}\mathcal{F}_{gt} + \mathcal{F}_{wt})) + \mathcal{F}_{gt}(\mathcal{F}_{tr}(1 - \mathcal{F}_{wg}\mathcal{F}_{gw}) + \mathcal{F}_{wr}(\mathcal{F}_{tg}\mathcal{F}_{gw} + \mathcal{F}_{tw}))}{\mathcal{D}} \right) R_0 \\
& + \left(1 + \frac{\mathcal{F}_{gw}(\mathcal{F}_{wg}(1 - \mathcal{F}_{tr}\mathcal{F}_{rt}) + \mathcal{F}_{tg}(\mathcal{F}_{wr}\mathcal{F}_{rt} + \mathcal{F}_{wt})) + \mathcal{F}_{gt}(\mathcal{F}_{tg}(1 - \mathcal{F}_{wr}\mathcal{F}_{rw} - \mathcal{F}_{ww}) + \mathcal{F}_{wg}(\mathcal{F}_{tr}\mathcal{F}_{rw} + \mathcal{F}_{tw}))}{\mathcal{D}} \right) G_0 \\
& + \left(\frac{\mathcal{F}_{gt}(\mathcal{F}_{tr}\mathcal{F}_{rw} + \mathcal{F}_{tg}\mathcal{F}_{gw} + \mathcal{F}_{tw}) + \mathcal{F}_{gw}(1 - \mathcal{F}_{tr}\mathcal{F}_{rt} - \mathcal{F}_{tg}\mathcal{F}_{gt})}{\mathcal{D}} \right) W_0
\end{aligned} \tag{C38}$$

15 The denominator is expressed as following:

$$\begin{aligned}
\mathcal{D} = & (1 - \mathcal{F}_{wr}\mathcal{F}_{rw} - \mathcal{F}_{wg}\mathcal{F}_{gw} - \mathcal{F}_{ww})(1 - \mathcal{F}_{tr}\mathcal{F}_{rt} - \mathcal{F}_{tg}\mathcal{F}_{gt}) \\
& - (\mathcal{F}_{wr}\mathcal{F}_{rt} + \mathcal{F}_{wg}\mathcal{F}_{gt} + \mathcal{F}_{wt})(\mathcal{F}_{tr}\mathcal{F}_{rw} + \mathcal{F}_{tg}\mathcal{F}_{gw} + \mathcal{F}_{tw})
\end{aligned} \tag{C39}$$

References

- Abdel-Aziz, D. M., Shboul, A. A., and Al-Kurdi, N. Y.: Effects of Tree Shading on Building's Energy Consumption -The Case of Residential Buildings in a Mediterranean Climate, *American Journal of Environmental Engineering*, 5, 131–140, doi:10.5923/j.ajee.20150505.01, 2015.
- Akbari, H., Kurn, D. M., Bretz, S. E., and Hanford, J. W.: Peak power and cooling energy savings of shade trees, *Energy and Buildings*, 25, 139–148, 1997.
- Akbari, H., Pomerantz, M., and Taha, H.: Cool surfaces and shade trees to reduce energy use and improve air quality in urban areas, *Solar Energy*, 70, 295–310, doi:10.1016/S0038-092X(00)00089-X, 2001.
- Alavipanah, S., Wegmann, M., Qureshi, S., Weng, Q., and Koellner, T.: The Role of Vegetation in Mitigating Urban Land Surface Temperatures: A Case Study of Munich, Germany during the Warm Season, *Sustainability*, 7, 4689–4706, doi:10.3390/su7044689, <http://www.mdpi.com/2071-1050/7/4/4689/>, 2015.
- Alvey, A. A.: Promoting and preserving biodiversity in the urban forest, *Urban Forestry and Urban Greening*, 5, 195–201, doi:10.1016/j.ufug.2006.09.003, 2006.
- Armson, D., Stringer, P., and Ennos, A. R.: The effect of street trees and amenity grass on urban surface water runoff in Manchester, UK, *Urban Forestry and Urban Greening*, 12, 282–286, doi:10.1016/j.ufug.2013.04.001, <http://dx.doi.org/10.1016/j.ufug.2013.04.001>, 2013.
- Barcelona City Council: Street Tree Management in Barcelona, Tech. rep., 2011.
- Bertram, C. and Rehdanz, K.: The role of urban green space for human well-being, 2014.
- Boone, A., Calvet, J.-C., and Noilhan, J.: Inclusion of a Third Soil Layer in a Land Surface Scheme Using the Force–Restore Method, *Journal of Applied Meteorology*, 38, 1611–1630, doi:10.1175/1520-0450(1999)038<1611:IOATSL>2.0.CO;2, 1999.
- Bouyer, J., Inard, C., and Musy, M.: Microclimatic coupling as a solution to improve building energy simulation in an urban context, *Energy and Buildings*, 43, 1549–1559, doi:10.1016/j.enbuild.2011.02.010, <http://linkinghub.elsevier.com/retrieve/pii/S0378778811000545>, 2011.
- Bowen, K. J. and Parry, M.: The evidence base for linkages between green infrastructure, public health and economic benefit, Tech. rep., 2015.
- Bruse, M. and Fleer, H.: Simulating surface-plant-air interactions inside urban environments with a three dimensional numerical model, *Environmental Modelling and Software*, 13, 373–384, doi:10.1016/S1364-8152(98)00042-5, 1998.
- Campbell, G. S. and Norman, J. M.: The description and measurement of plant canopy structure, UK: Cambridge University Press, 1989.
- City of Westminster: Trees and the Public Realm (Draft), Tech. Rep. December, 2009.
- Coutts, A. M., White, E. C., Tapper, N. J., Beringer, J., and Livesley, S. J.: Temperature and human thermal comfort effects of street trees across three contrasting street canyon environments, *Theoretical and Applied Climatology*, pp. 1–14, doi:10.1007/s00704-015-1409-y, <http://link.springer.com/10.1007/s00704-015-1409-y>, 2015.
- de Abreu-Harbach, L. V., Labaki, L. C., and Matzarakis, A.: Effect of tree planting design and tree species on human thermal comfort in the tropics, *Landscape and Urban Planning*, 138, 99–109, doi:10.1016/j.landurbplan.2015.02.008, <http://linkinghub.elsevier.com/retrieve/pii/S0169204615000390>, 2015.
- De Blichambaut, C. P.: Rayonnement solaire et échanges radiatifs naturels: méthodes actinométriques, Gauthier-Villars, 1963.
- de Munck, C.: Modélisation de la végétation urbaine et stratégies d'adaptation pour l'amélioration du confort climatique et de la demande énergétique en ville, Ph.D. thesis, Université Toulouse III, <http://oatao.univ-toulouse.fr/9278/>, 2013.

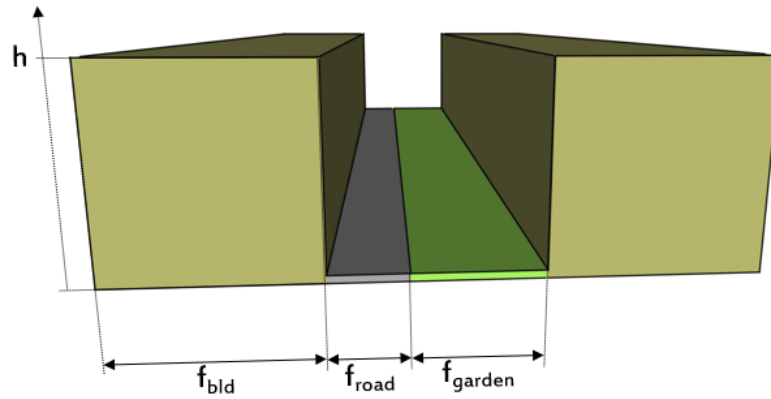
- Feyisa, G. L., Dons, K., and Meilby, H.: Efficiency of parks in mitigating urban heat island effect: An example from Addis Ababa, *Landscape and Urban Planning*, 123, 87–95, doi:10.1016/j.landurbplan.2013.12.008, <http://linkinghub.elsevier.com/retrieve/pii/S0169204613002399>, 2014.
- Grimmond, C. S. B., Blackett, M., Best, M. J., Baik, J.-J., Belcher, S. E., Beringer, J., Bohnenstengel, S. I., Calmet, I., Chen, F., Coutts, A., Dandou, A., Fortuniak, K., Gouvea, M. L., Hamdi, R., Hendry, M., Kanda, M., Kawai, T., Kawamoto, Y., Kondo, H., Krayenhoff, E. S., Lee, S.-H., Loridan, T., Martilli, A., Masson, V., Miao, S., Oleson, K., Ooka, R., Pigeon, G., Porson, A., Ryu, Y.-H., Salamanca, F., Steeneveld, G., Tombrou, M., Voogt, J. A., Young, D. T., and Zhang, N.: Initial results from Phase 2 of the international urban energy balance model comparison, *International Journal of Climatology*, 31, 244–272, doi:10.1002/joc.2227, <http://onlinelibrary.wiley.com/doi/10.1002/joc.2227/full><http://doi.wiley.com/10.1002/joc.2227>, 2011.
- Groleau, D. and Mestayer, P. G.: Urban Morphology Influence on Urban Albedo: A Revisit with the SOLENE Model, *Boundary-Layer Meteorology*, 147, 301–327, doi:10.1007/s10546-012-9786-6, 2013.
- Hamdi, R. and Masson, V.: Inclusion of a Drag Approach in the Town Energy Balance (TEB) Scheme: Offline 1D Evaluation in a Street Canyon, *Journal of Applied Meteorology and Climatology*, 47, 2627–2644, doi:10.1175/2008JAMC1865.1, <http://journals.ametsoc.org/doi/abs/10.1175/2008JAMC1865.1>, 2008.
- Harman, I. N. and Belcher, S. E.: The surface energy balance and boundary layer over urban street canyons, *Quarterly Journal of the Royal Meteorological Society*, 132, 2749–2768, doi:10.1256/qj.05.185, <http://doi.wiley.com/10.1256/qj.05.185>, 2006.
- Hien, W. N., Puay Yok, T. P., and Yu, C.: Study of thermal performance of extensive rooftop greenery systems in the tropical climate, *Building and Environment*, 42, 25–54, doi:10.1016/j.buildenv.2005.07.030, <http://linkinghub.elsevier.com/retrieve/pii/S0360132305003136>, 2007.
- Hottel, H. C.: Radiant-Heat Transmission, in: *Heat Transmission*, edited by Mc Adams, W. H., pp. 55–125, Mc Graw-Hill, 1954.
- Jim, C. Y.: Air-conditioning energy consumption due to green roofs with different building thermal insulation, *Applied Energy*, 128, 49–59, doi:10.1016/j.apenergy.2014.04.055, <http://linkinghub.elsevier.com/retrieve/pii/S0306261914004085>, 2014.
- Joshi, N. and Joshi, A.: Role of Urban Trees in Amelioration of Temperatures, *International Journal of Research Studies in Biosciences*, 3, 132–137, 2015.
- Ko, Y., Lee, J.-H., McPherson, E. G., and Roman, L. a.: Long-term monitoring of Sacramento Shade program trees: Tree survival, growth and energy-saving performance, *Landscape and Urban Planning*, 143, 183–191, doi:10.1016/j.landurbplan.2015.07.017, <http://linkinghub.elsevier.com/retrieve/pii/S0169204615001553>, 2015.
- Kokogiannakis, G., Tietje, A., and Darkwa, J.: The role of Green Roofs on Reducing Heating and Cooling Loads: A Database across Chinese Climates, *Procedia Environmental Sciences*, 11, 604–610, doi:10.1016/j.proenv.2011.12.094, <http://linkinghub.elsevier.com/retrieve/pii/S1878029611009170>, 2011.
- Kounkou-Arnaud, R., Desplat, J., Lemonsu, A., and Salagnac, J.-L.: Epicea : étude des impacts du changement climatique à Paris, *La Météorologie*, 8, 42–48, doi:10.4267/2042/53186, <http://hdl.handle.net/2042/53186>, 2014.
- Krayenhoff, E. S., Christen, A., Martilli, A., and Oke, T. R.: A Multi-layer Radiation Model for Urban Neighbourhoods with Trees, *Boundary-Layer Meteorology*, 151, 139–178, doi:10.1007/s10546-013-9883-1, <http://link.springer.com/10.1007/s10546-013-9883-1>, 2014.
- Krayenhoff, E. S., Santiago, J. L., Martilli, A., Christen, A., and Oke, T. R.: Parametrization of Drag and Turbulence for Urban Neighbourhoods with Trees, *Boundary-Layer Meteorology*, 156, 157–189, doi:10.1007/s10546-015-0028-6, "<http://dx.doi.org/10.1007/s10546-015-0028-6>", 2015.

- Lafore, J. P., Stein, J., Asencio, N., Bougeault, P., Ducrocq, V., Duron, J., Fischer, C., H??reil, P., Mascart, P., Masson, V., Pinty, J. P., Redelsperger, J. L., Richard, E., and Vil??-Guerau De Arellano, J.: The Meso-NH Atmospheric Simulation System. Part I: Adiabatic
20 formulation and control simulations, *Annales Geophysicae*, 16, 90–109, doi:10.1007/s005850050582, 1997.
- Lee, S.-H. and Park, S.-U.: A Vegetated Urban Canopy Model for Meteorological and Environmental Modelling, *Boundary-Layer Meteorology*, 126, 73–102, doi:10.1007/s10546-007-9221-6, <http://link.springer.com/10.1007/s10546-007-9221-6>, 2008.
- Lemonsu, A., Grimmond, C. S. B., and Masson, V.: Modeling the Surface Energy Balance of the Core of an Old Mediterranean City: Marseille, *Journal of Applied Meteorology*, 43, 312–327, 2004.
- 25 Lemonsu, A., Bélair, S., Mailhot, J., and Leroyer, S.: Evaluation of the Town Energy Balance model in cold and snowy conditions during the Montreal Urban Snow Experiment 2005, *Journal of Applied Meteorology and Climatology*, 49, 346–362, doi:10.1175/2009JAMC2131.1, 2010.
- Lemonsu, A., Masson, V., Shashua-Bar, L., Erell, E., and Pearlmutter, D.: Inclusion of vegetation in the Town Energy Balance model for modelling urban green areas, *Geoscientific Model Development*, 5, 1377–1393, doi:10.5194/gmd-5-1377-2012, <http://www.geosci-model-dev.net/5/1377/2012/>, 2012.
- 30 Lemonsu, A., Koukou-Arnaud, R., Desplat, J., Salagnac, J.-L., and Masson, V.: Evolution of the Parisian urban climate under a global changing climate, *Climatic Change*, 116, 679–692, doi:10.1007/s10584-012-0521-6, <http://link.springer.com/10.1007/s10584-012-0521-6>, 2013.
- Malys, L.: Modélisation de la végétation urbaine et stratégies d’adaptation pour l’amélioration du confort climatique et de la demande
35 énergétique en ville, Ph.D. thesis, Ecole Centrale de Nantes, France, 2012.
- Malys, L., Musy, M., and Inard, C.: A hydrothermal model to assess the impact of green walls on urban microclimate and building energy consumption, *Building and Environment*, 73, 187–197, doi:10.1016/j.buildenv.2013.12.012, <http://linkinghub.elsevier.com/retrieve/pii/S0360132313003685>, 2014.
- Masson, V.: A physically-based scheme for the urban energy budget in atmospheric models, *Boundary-Layer Meteorology*, 94, 357–397, 2000.
- Masson, V. and Seity, Y.: Including Atmospheric Layers in Vegetation and Urban Offline Surface Schemes, *Journal of Applied Meteorology
5 and Climatology*, 48, 1377–1397, doi:10.1175/2009JAMC1866.1, <http://journals.ametsoc.org/doi/abs/10.1175/2009JAMC1866.1>, 2009.
- Masson, V., Grimmond, C. S. B., and Oke, T. R.: Evaluation of the Town Energy Balance (TEB) Scheme with Direct Measurements from Dry Districts in Two Cities, *Journal of Applied Meteorology*, 41, 1011–1026, 2002.
- Masson, V., Le Moigne, P., Martin, E., Faroux, S., Alias, A., Alkama, R., Belamari, S., Barbu, A., Boone, A., Bouysse, F., Brousseau, P., Brun, E., Calvet, J.-C., Carrer, D., Decharme, B., Delire, C., Donier, S., Essaouini, K., Gibelin, A.-L., Giordani, H., Habets, F., Jidane, M.,
10 Kerdraon, G., Kourzeneva, E., Lafaysse, M., Lafont, S., Lebeaupin Brossier, C., Lemonsu, A., Mahfouf, J.-F., Marguinaud, P., Mokhtari, M., Morin, S., Pigeon, G., Salgado, R., Seity, Y., Taillefer, F., Tanguy, G., Tulet, P., Vincendon, B., Vionnet, V., and Voldoire, A.: The SURFEXv7.2 land and ocean surface platform for coupled or offline simulation of earth surface variables and fluxes, *Geoscientific Model Development*, 6, 929–960, doi:10.5194/gmd-6-929-2013, <http://www.geosci-model-dev.net/6/929/2013/>, 2013.
- Miguet, F.: Paramètres physiques des ambiances architecturales : Un modèle numérique pour la simulation de la lumière naturelle dans le
15 projet urbain, Ph.D. thesis, <https://tel.archives-ouvertes.fr/tel-00546996/>, 2000.
- Miguet, F. and Groleau, D.: A daylight simulation tool for urban and architectural spaces-application to transmitted direct and diffuse light through glazing, *Building and Environment*, 37, 833–843, doi:10.1016/S0360-1323(02)00049-5, 2002.

- Mullaney, J., Lucke, T., and Trueman, S. J.: A review of benefits and challenges in growing street trees in paved urban environments, *Landscape and Urban Planning*, 134, 157–166, doi:10.1016/j.landurbplan.2014.10.013, 2015.
- 20 Municipality of Toulouse: CAHIER DE L'ESPACE PUBLIC « LES ESPACES VERTS », Tech. rep., Toulouse, France, 2008.
- Noilhan, J. and Planton, S.: A Simple Parameterization of Land Surface Processes for Meteorological Models, *Monthly Weather Review*, 117, 536–549, 1989.
- Nowak, D. J. and Dwyer, J. F.: Understanding the Benefits and Costs of Urban Forest Ecosystems, in: *Handbook of Urban and Community Forestry in the North East*, pp. 25–46, doi:10.1007/978-1-4020-4289-8_2, 2007.
- 25 Önder, S. and Akay, A.: The Roles of Plants on Mitigating the Urban Heat Islands' Negative Effects, *International Journal of Agriculture and Economic Development*, 2, 18–32, 2014.
- Park, M., Hagishima, A., Tanimoto, J., and Narita, K. I.: Effect of urban vegetation on outdoor thermal environment: Field measurement at a scale model site, *Building and Environment*, 56, 38–46, doi:10.1016/j.buildenv.2012.02.015, <http://dx.doi.org/10.1016/j.buildenv.2012.02.015>, 2012.
- 30 Perez, R., Seals, R., and Michalsky, J.: All-weather model for sky luminance distribution-Preliminary configuration and validation, *Solar Energy*, 50, 235–245, doi:10.1016/0038-092X(93)90017-I, 1993.
- Pigeon, G., Moscicki, M. A., Voogt, J. A., and Masson, V.: Simulation of fall and winter surface energy balance over a dense urban area using the TEB scheme, *Meteorology and Atmospheric Physics*, 102, 159–171, 2008.
- Porson, A., Harman, I. N., Bohnenstengel, S. I., and Belcher, S. E.: How many facets are needed to represent the surface energy balance of an urban area?, *Boundary-Layer Meteorology*, 132, 107–128, doi:10.1007/s10546-009-9392-4, 2009.
- 35 Qiu, G. Y., Li, H. Y., Zhang, Q. T., Chen, W., Liang, X. J., and Li, X. Z.: Effects of Evapotranspiration on Mitigation of Urban Temperature by Vegetation and Urban Agriculture, *Journal of Integrative Agriculture*, 12, 1307–1315, doi:10.1016/S2095-3119(13)60543-2, 2013.
- Robitu, M., Musy, M., Inard, C., and Groleau, D.: Modeling the influence of vegetation and water pond on urban microclimate, *Solar Energy*, 80, 435–447, doi:10.1016/j.solener.2005.06.015, <http://linkinghub.elsevier.com/retrieve/pii/S0038092X05002574>, 2006.
- Ryu, Y. H., Bou-Zeid, E., Wang, Z. H., and Smith, J. A.: Realistic Representation of Trees in an Urban Canopy Model, *Boundary-Layer Meteorology*, pp. 1–28, doi:10.1007/s10546-015-0120-y, 2015.
- 5 Seity, Y., Brousseau, P., Malardel, S., Hello, G., Bénard, P., Bouttier, F., Lac, C., and Masson, V.: The AROME-France Convective-Scale Operational Model, *Monthly Weather Review*, 139, 976–991, doi:10.1175/2010MWR3425.1, <http://journals.ametsoc.org/doi/abs/10.1175/2010MWR3425.1>, 2011.
- Shashua-Bar, L., Pearlmutter, D., and Erell, E.: The influence of trees and grass on outdoor thermal comfort in a hot-arid environment, *International Journal of Climatology*, 31, 1498–1506, doi:10.1002/joc.2177, 2011.
- 10 Simpson, J. R.: Improved estimates of tree-shade effects on residential energy use, *Energy and Buildings*, 34, 1067–1076, doi:10.1016/S0378-7788(02)00028-2, 2002.
- Spangenberg, J., Shinzato, P., Johansson, E., and Duarte, D. H. S.: Simulation of the influence of vegetation on microclimate and thermal comfort in the city of São Paulo, *Revista da Sociedade Brasileira de Arborização Urbana*, 3, 1–19, doi:10.1016/j.solener.2005.06.015, 2008.
- 15 Taleghani, M., Sailor, D., and Ban-Weiss, G. A.: Micrometeorological simulations to predict the impacts of heat mitigation strategies on pedestrian thermal comfort in a Los Angeles neighborhood, *Environ. Res. Lett.*, 11, 024003, doi:10.1088/1748-9326/11/2/024003, <http://iopscience.iop.org/1748-9326/11/2/024003>, 2016.

- Tavares, R., Calmet, I., and Dupont, S.: Modelling the impact of green infrastructures on local microclimate within an idealized homogeneous urban canopy, in: ICUC9 - 9th International Conference on Urban Climate jointly with 12th Symposium on the Urban Environment Modelling, pp. 1–6, 2015.
- 5 Wang, Z.-H.: Monte Carlo simulations of radiative heat exchange in a street canyon with trees, *Solar Energy*, 110, 704–713, doi:10.1016/j.solener.2014.10.012, <http://www.sciencedirect.com/science/article/pii/S0038092X14004988>, 2014.
- Yamada, T.: A numerical study of turbulent airflow in and above a forest canopy, *Journal of the Meteorological Society of Japan*, 60, 439–454, 1065 1982.
- Yao, L., Chen, L., Wei, W., and Sun, R.: Potential reduction in urban runoff by green spaces in Beijing: A scenario analysis, *Urban Forestry & Urban Greening*, 14, 300–308, doi:10.1016/j.ufug.2015.02.014, <http://linkinghub.elsevier.com/retrieve/pii/S1618866715000369>, 2015.
- Young, D. T., Clark, P., Hendry, M., and Barlow, J.: Modelling Radiative Exchange in a Vegetated Urban Street Canyon Model, in: ICUC9 - 9th International Conference on Urban Climate jointly with 12th Symposium on the Urban Environment Modelling, pp. 1–5, 2015.
- 1070 Zhang, B., Xie, G.-d., Li, N., and Wang, S.: Effect of urban green space changes on the role of rainwater runoff reduction in Beijing, China, *Landscape and Urban Planning*, 140, 8–16, doi:10.1016/j.landurbplan.2015.03.014, <http://linkinghub.elsevier.com/retrieve/pii/S0169204615000766>, 2015.
- Zhang, Z., Lv, Y., and Pan, H.: Cooling and humidifying effect of plant communities in subtropical urban parks, *Urban Forestry and Urban Greening*, 12, 323–329, doi:10.1016/j.ufug.2013.03.010, 2013.

a. Without explicit high vegetation



b. With explicit high vegetation

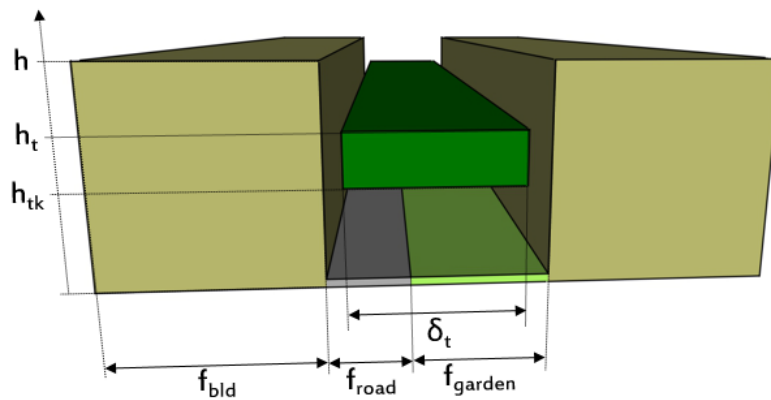


Figure 1. Comparison of the spatial arrangement of elements composing the urban canyon and of associated geometric parameters applied in the TEB model in the reference case (top) and in the case with explicit high vegetation (bottom).

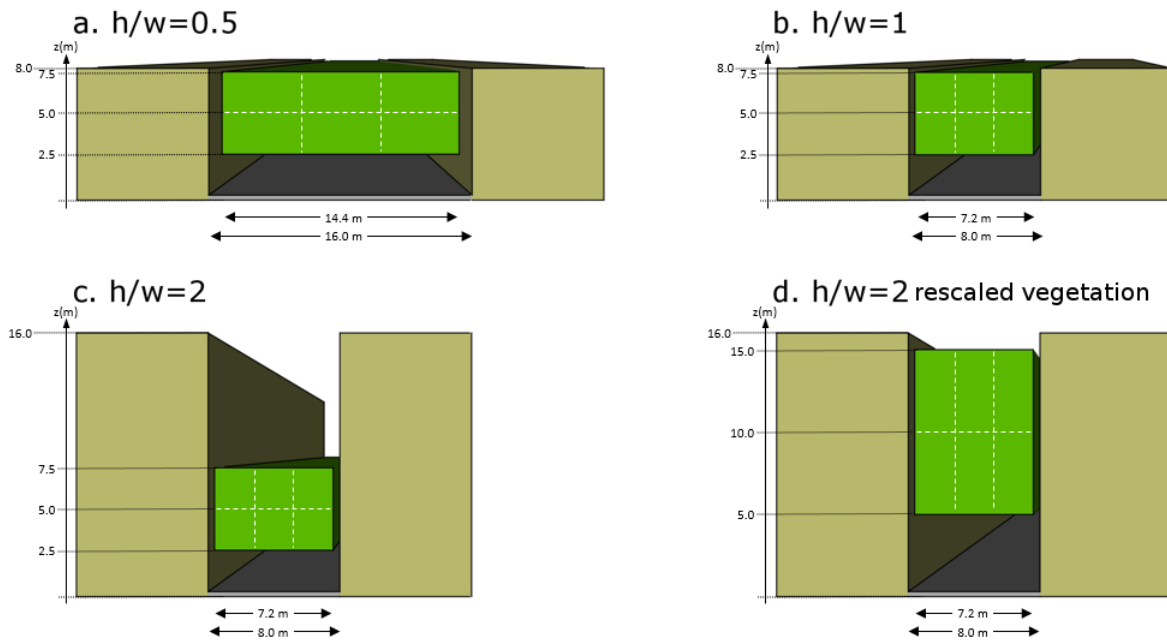


Figure 2. Description of simple geometries of urban canyon selected for the comparison between TEB and ~~SOLENE~~ SOLENE simulations. For each of them, the potential location of tree canopy is illustrated by dotted rectangles.

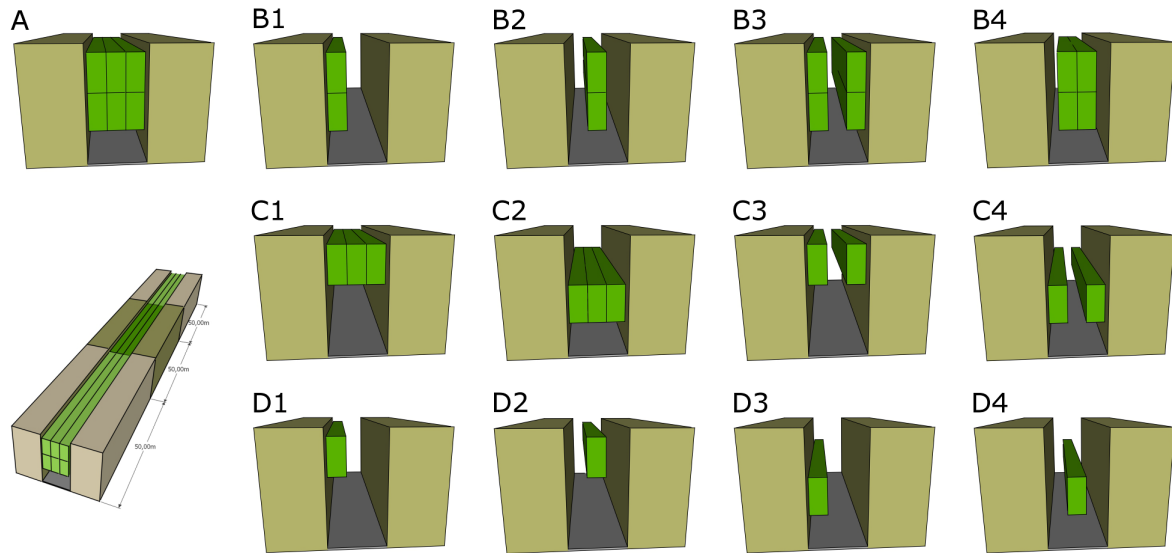


Figure 3. Description of the SOLENE-SOLENE mock-up, and presentation of the ensemble of vegetation layouts selected for the comparison between TEB and SOLENE-SOLENE simulations. The cases are presented here for the example of urban canyon with $h/w=2$ rescaled vegetation (see section 5.2.1 and doubled-thickness-of-crowns Fig. 2 for further explanations).

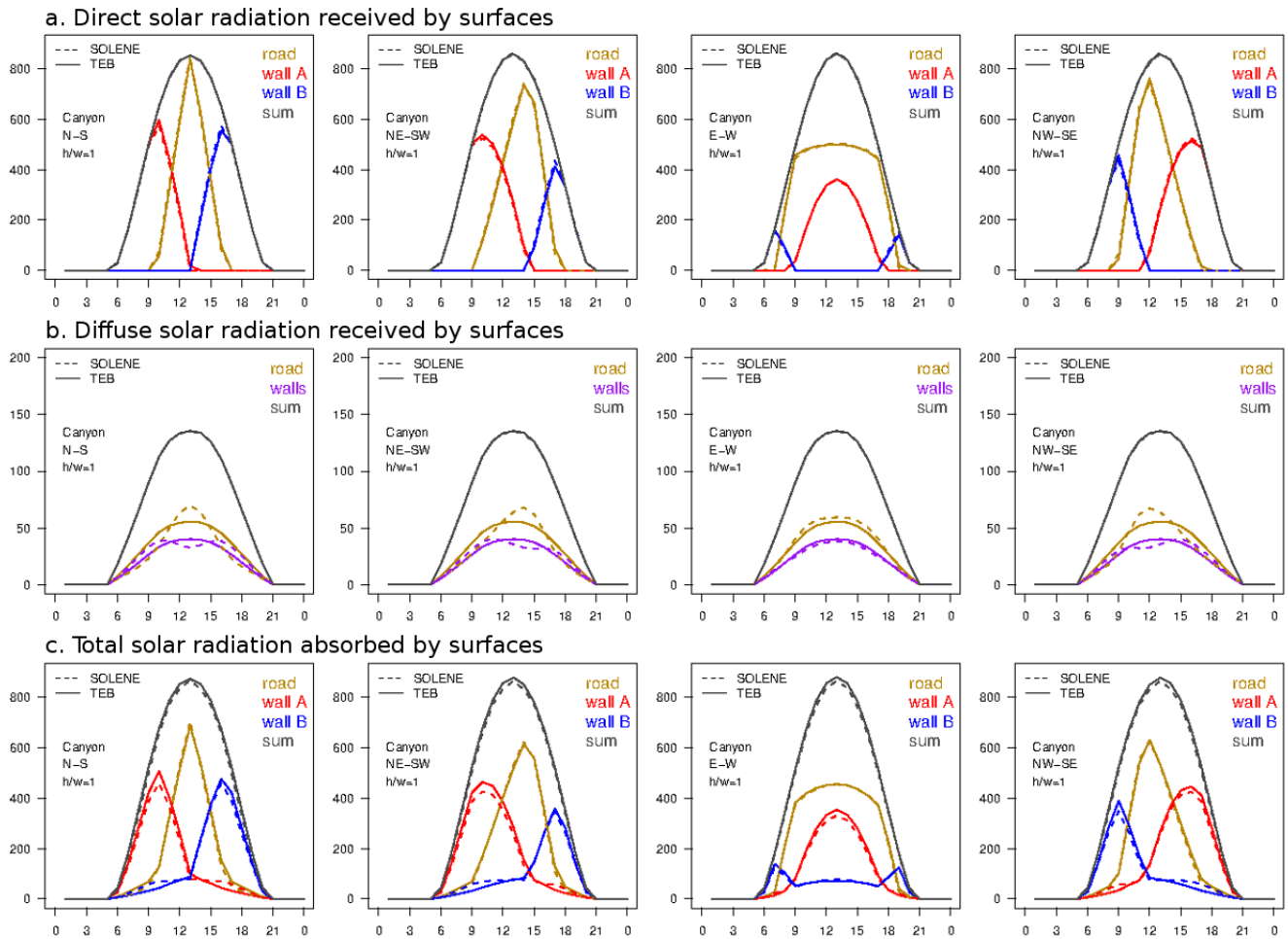


Figure 4. Comparison of TEB and SOLENE-SOLENE simulations of hourly direct (top) and diffuse (middle) solar radiation fluxes ($W m^{-2}$) received by urban facets before multiple reflections and total solar-shortwave radiation fluxes ($W m^{-2}$) absorbed by urban facets after interreflections (bottom), for urban canyons without vegetation. The results are presented here only for the aspect ratio equal to 1 and for the four street orientations at summertime.

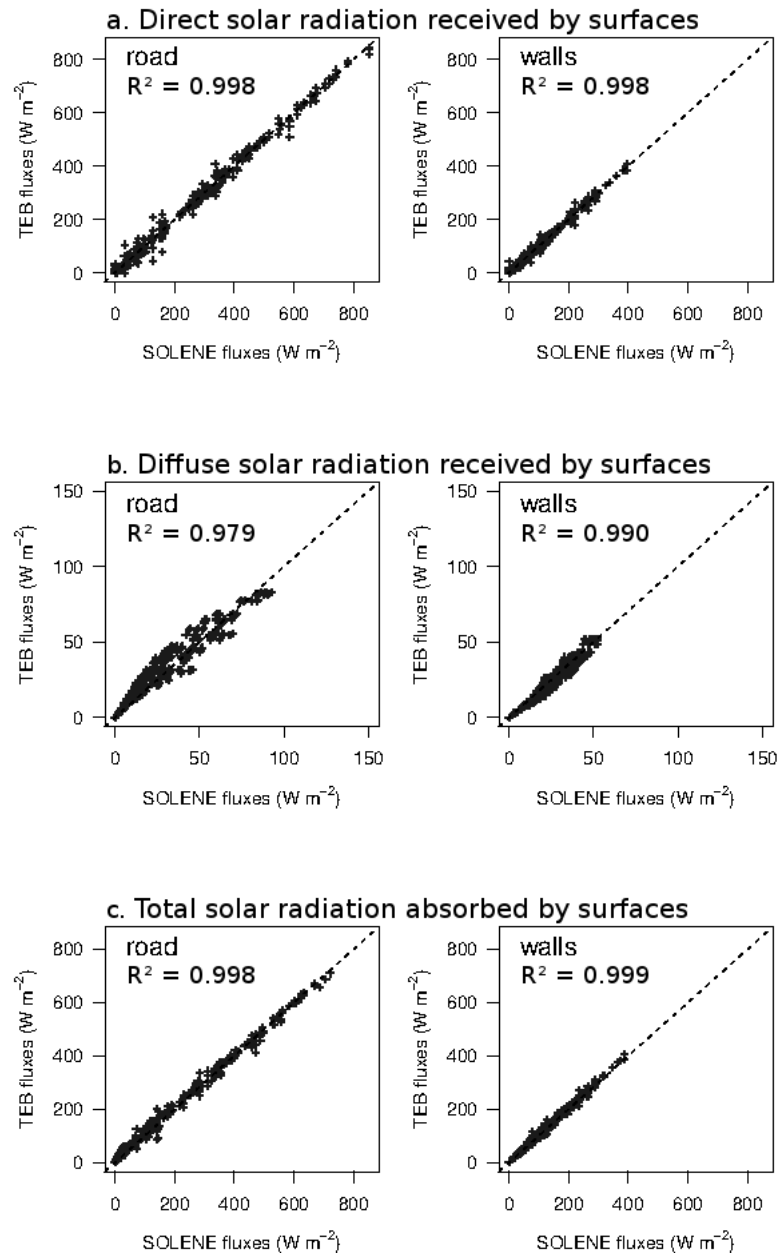


Figure 5. Scatterplots comparing TEB and **SOLENE-SOLENE** simulations of hourly direct (top) and diffuse (middle) solar radiation fluxes ($W m^{-2}$) received by urban facets before multiple reflections and total solar-shortwave radiation fluxes ($W m^{-2}$) absorbed by urban facets after interreflections (bottom), for urban canyons without vegetation. Each scatterplot gathers the hourly fluxes simulated for the four seasons, the three aspect ratios, and the four street orientations.

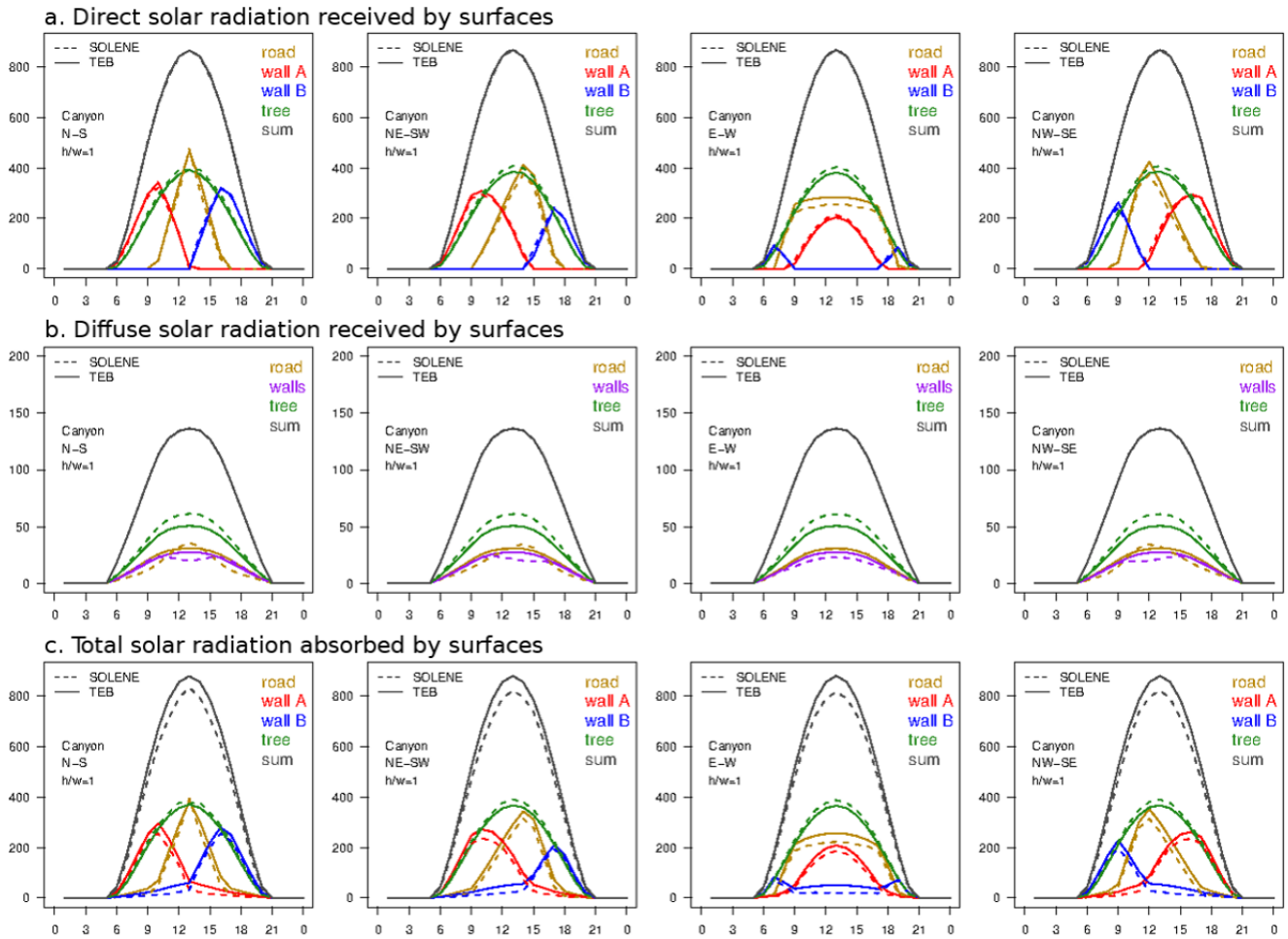


Figure 6. Comparison of TEB and SOLENE simulations of hourly direct (top) and diffuse (middle) solar radiation fluxes ($W m^{-2}$) received by urban facets before multiple reflections and total solar-shortwave radiation fluxes ($W m^{-2}$) absorbed by urban facets after interreflections (bottom), for urban canyons with vegetation. The results are presented here only for the aspect ratio equal to 1 and for the four street orientations at summertime.

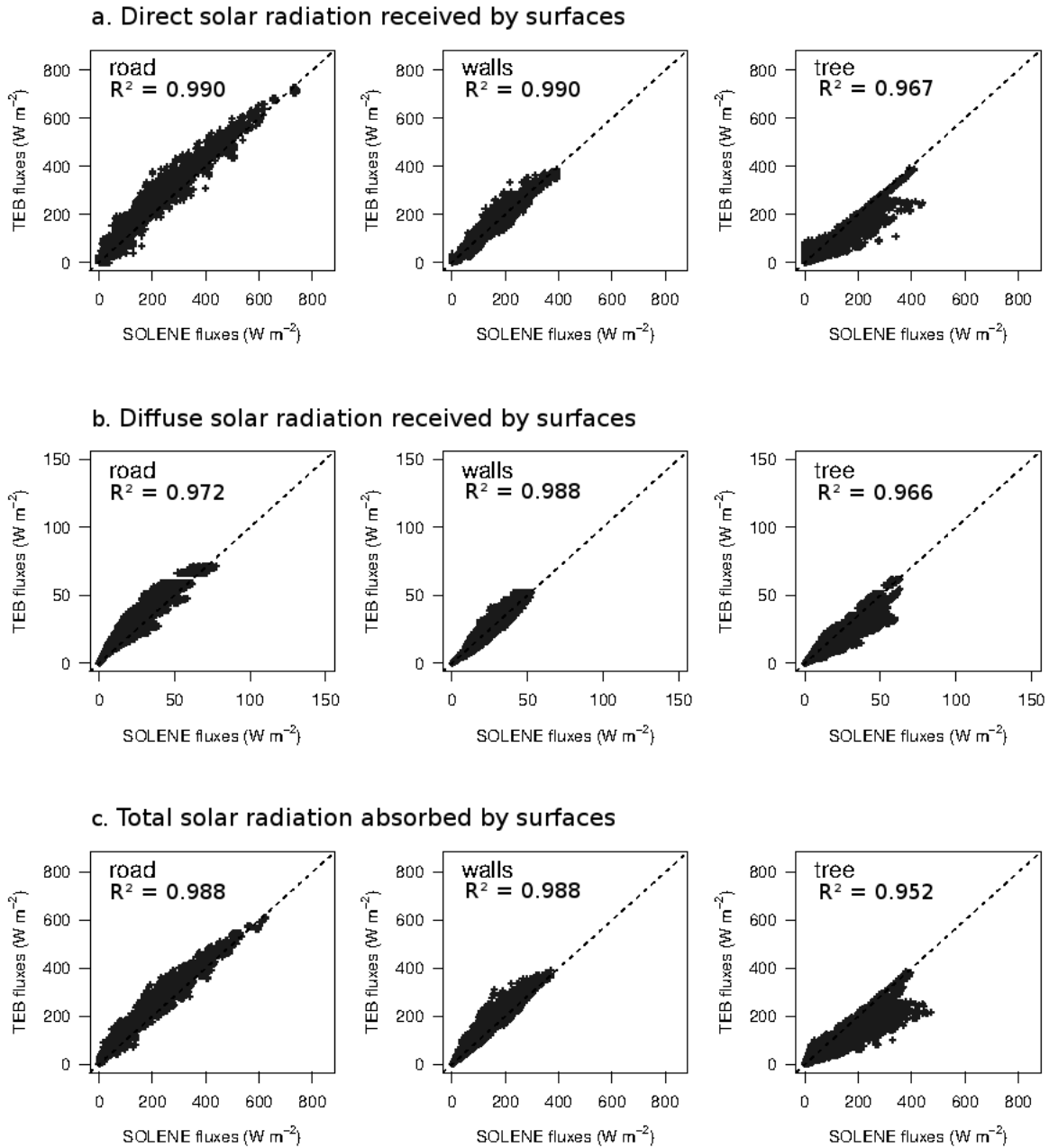


Figure 7. Scatterplots comparing TEB and [SOLENE-SOLENE](#) simulations of hourly direct (top) and diffuse (middle) solar radiation [fluxes \(\$W m^{-2}\$ \)](#) received by facets before [multiple](#) reflections and total [solar-shortwave](#) radiation [fluxes \(\$W m^{-2}\$ \)](#) absorbed by facets after inter-reflections (bottom), for urban canyons with vegetation. Each scatterplot gathers the hourly fluxes simulated for the four seasons, the four aspect ratios, and the four street orientations.

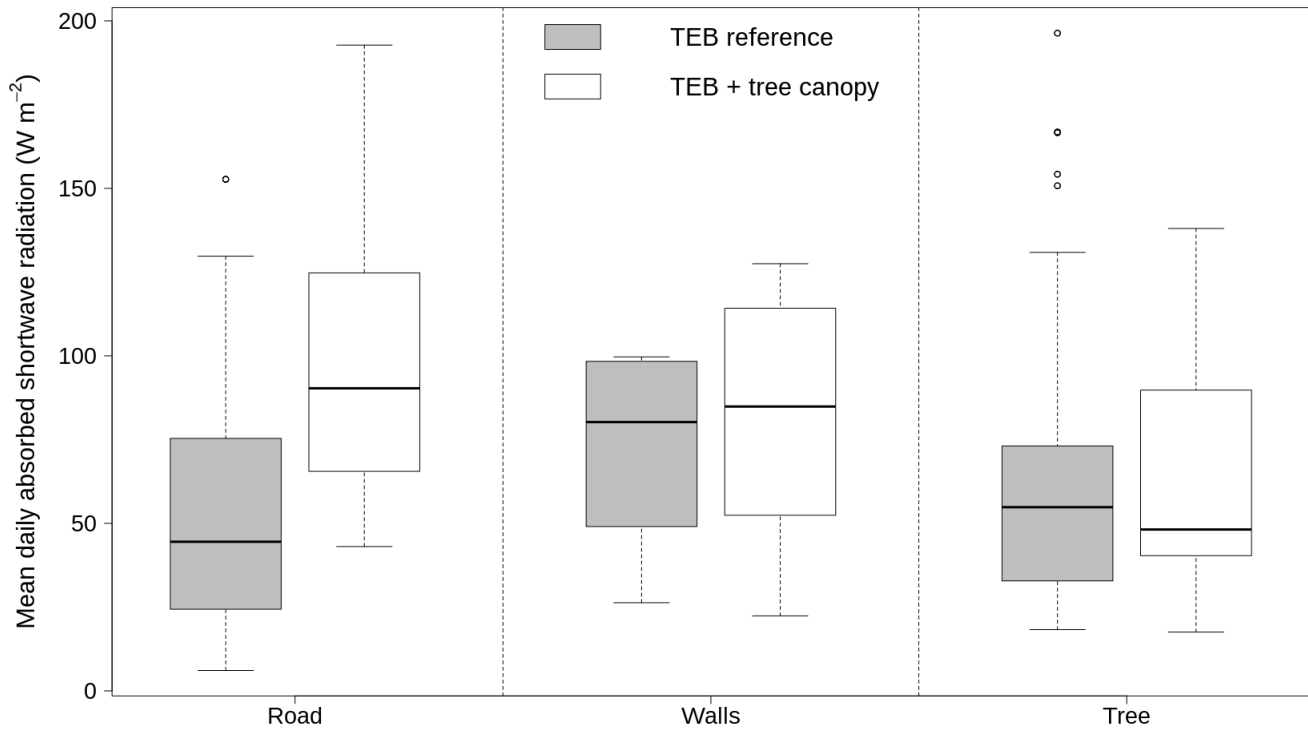


Figure 8. Effect Comparison of horizontal cover fraction of mean daily total shortwave radiation flux ($W m^{-2}$) absorbed by road, walls, and tree canopy on relative error between the reference TEB simulations without distinction between low and root-mean-squared error. Vegetation layouts are classified in three groups according to high vegetation and the cover fraction: 30% new version including a tree canopy by surface for layouts B1 all seasons, B2 aspect ratios, D1, D2, D3, D4; 60% for layouts B3, B4, C3, C4; orientations and 90% for vegetation layouts A, C1, C2 confounded.

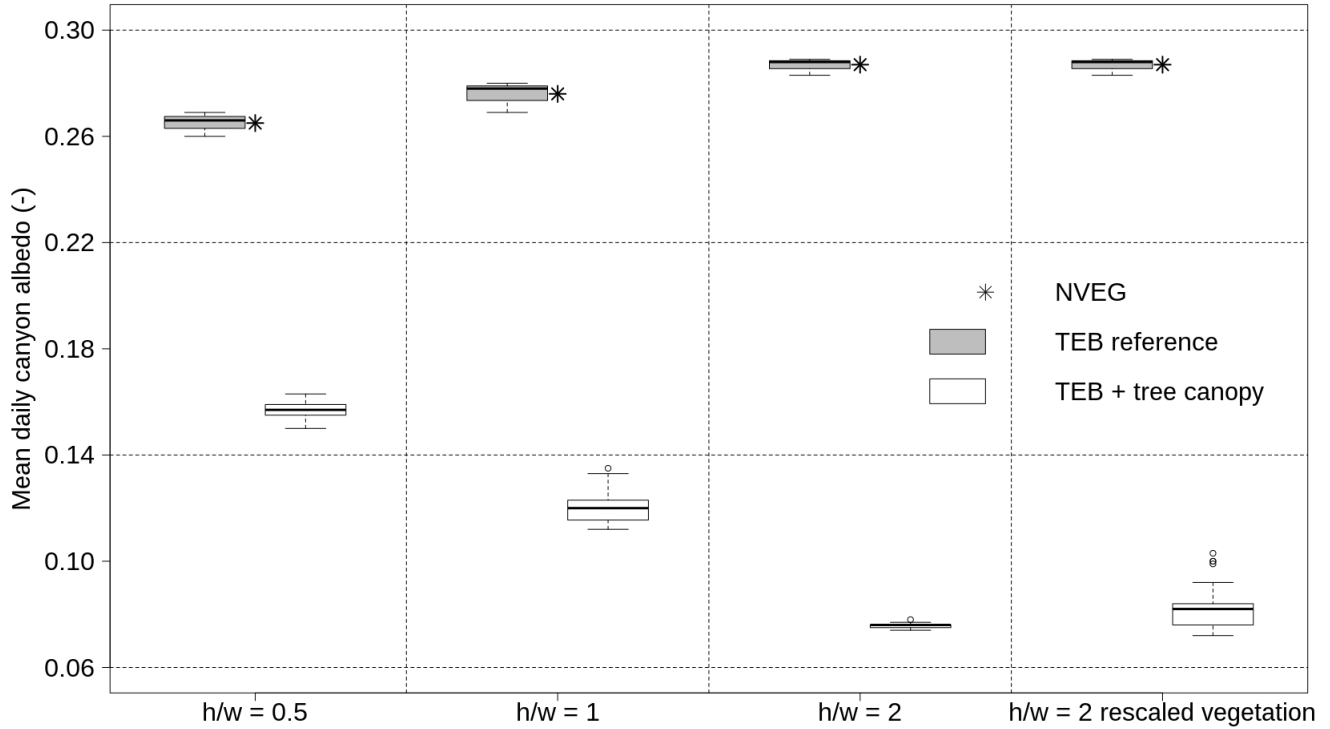


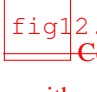


Figure 9. Effect Comparison of location of tree canopy on the vertical plane on relative error and root mean squared error. Vegetation layouts are classified in three groups: *Bottom* when the foliage is in the middle part of the daily canyon (layouts C2, C4, D3, D4); *Top* when albedo between the foliage is in the higher part of the canyon (layouts C1, C3, D1, D2); reference TEB simulations without distinction between low and All when the foliage extends in the high half of vegetation and the canyon (layouts A new version including a tree canopy by aspect ratios for all seasons, B1, B2, B3, B4) orientations and vegetation layouts confounded. See section 5.2.1 and Fig. 2 for further explanations about the $h/w = 2$ rescaled vegetation configurations.

Table 1. Main descriptive parameters of the urban canyon, including vegetation, in the TEB model. The bold parameters are the input data prescribed by user, the other ones are computed in the model using the input parameters.

Parameters	Symbol	Unit
Cover fraction of buildings	f_{bld}	-
Cover fraction of ground-based natural covers (garden)	f_{garden}	-
Proportion of bare soil in gardens	δ_{nv}	-
Proportion of low vegetation in gardens	$\delta_{lv} = 1 - \delta_{nv}$	-
Cover fraction of tree canopy	δ_t	-
Mean building height	h	m
Wall plan area ratio	r_w	-
Canyon aspect ratio	$h/w = 0.5r_w/(1 - f_{\text{bld}})$	-
Height of tree canopy	h_t	m
Height of trunk	h_{tk}	m
Mid-height of tree's crown	$h_{cw} = (h_t + h_{tk})/2$	m
Sky-view Sky view factor of wall, road, garden, tree	$\Psi_{ws}, \Psi_{rs}, \Psi_{gs}, \Psi_{ts}$	-
View factor of road, tree from wall	Ψ_{wr}, Ψ_{wt}	-
View factor of wall, tree from road	Ψ_{rw}, Ψ_{rt}	-
View factor of wall,road from tree	Ψ_{tw}, Ψ_{tr}	-
Leaf Area Index of low vegetation in gardens	LAI_g	m^2m^{-2}
Leaf Area Index of tree canopy	LAI_t	m^2m^{-2}
Leaf Area Density of tree canopy	LAD_t	m^3m^{-2} m^2m^{-3}
Albedo of wall, road, garden, tree	$\alpha_w, \alpha_r, \alpha_g, \alpha_t$	-
Emissivity of wall, road, garden, tree	$\epsilon_w, \epsilon_r, \epsilon_g, \epsilon_t$	-

1075  Effect of location of tree canopy on the horizontal plane on relative error and root-mean squared error. Vegetation layouts are classified in three groups: *Center* when the foliage is centered along the canyon axis (layouts A, B2, B4, C1, C2, D2, D4); *Edge* when the foliage is on the edge of the canyon (layouts B1, D1, D3); and *Double* when the foliage is separated in two lines (layouts B3, C3, C4).  Comparison of the mean daily canyon albedo between TEB and SOLENE models by aspect ratios for all orientations and vegetation layouts confounded at summertime.  Comparison of mean daily total solar radiation absorbed by road, walls, and tree between the reference TEB simulation without explicit high-vegetation and the new version including a tree canopy:

1080

Table 2. List of input parameters for the ensemble of simulations performed with TEB.

Parameters	A	B1	B2	B3	B4	C1	C2	C3	C4	D1	D2	D3	D4
f_{bld}	0.5	0.5	0.5	0.5	0.5	0.5	0.5	0.5	0.5	0.5	0.5	0.5	0.5
f_{garden}	0.	0.	0.	0.	0.	0.	0.	0.	0.	0.	0.	0.	0.
δ_t	0.9	0.3	0.3	0.6	0.6	0.9	0.9	0.6	0.6	0.3	0.3	0.3	0.3
h	8. (for $h/w = 0.5$, $h/w = 1$, $h/w = 2$ -classical case) / 16. (for $h/w = 2$ -rescaled vegetation)												
r_w	0.5 (for $h/w = 0.5$) / 1.0 (for $h/w = 1$) / 2.0 (for $h/w = 2$ -classical and rescaled vegetation cases)												
h_t	7.5	7.5	7.5	7.5	7.5	7.5	5.0	7.5	5.0	7.5	7.5	5.0	5.0
h_{tk}	2.5	2.5	2.5	2.5	2.5	5.0	2.5	5.0	2.5	5.0	5.0	2.5	2.5
LAI_t	<u>3-1.</u>	<u>3-1.</u>	<u>3-1.</u>	<u>3-1.</u>	<u>3-1.</u>	<u>3-1.</u>	<u>3-1.</u>	<u>3-1.</u>	<u>3-1.</u>	<u>3-1.</u>	<u>3-1.</u>	<u>3-1.</u>	<u>3-1.</u>
τ_{sr}	0.5	0.5	0.5	0.5	0.5	0.5	0.5	0.5	0.5	0.5	0.5	0.5	0.5
α_r	0.25	0.25	0.25	0.25	0.25	0.25	0.25	0.25	0.25	0.25	0.25	0.25	0.25
α_w	0.30	0.30	0.30	0.30	0.30	0.30	0.30	0.30	0.30	0.30	0.30	0.30	0.30
α_t	0.15	0.15	0.15	0.15	0.15	0.15	0.15	0.15	0.15	0.15	0.15	0.15	0.15

Table 3. Statistical scores for absorbed solar-shortwave radiation flux by surfaces regarding the seasons.

Config - Surf Units	Winter			Spring			Summer			Bias W m ⁻²
	<u>RMSE-MAE</u> W m ⁻²	<u>Err-MAPE</u> %	Bias W m ⁻²	<u>RMSE-MAE</u> W m ⁻²	<u>Err-MAPE</u> %	Bias W m ⁻²	<u>RMSE-MAE</u> W m ⁻²	<u>Err-MAPE</u> %		
NVEG										
Road	<u>4.35-2.13</u>	43	+2.02	<u>13.91-7.45</u>	18	+4.47	<u>9.88-6.03</u>	3	+3.50	
Walls	<u>1.94-0.81</u>	4	+0.42	<u>6.37-2.99</u>	2	+0.91	<u>5.72-3.38</u>	3	+2.80	
ALL										
Road	<u>5.41-2.67</u>	109	<u>+2.60-2.63</u>	<u>19.43-10.29</u>	64	<u>+9.12-9.21</u>	<u>26.44-16.26</u>	24	<u>+15.37-15.37</u>	
Walls	<u>5.01-1.93</u>	<u>14-15</u>	<u>+1.77-1.79</u>	<u>15.36-6.83</u>	<u>14-15</u>	<u>+5.39-5.47</u>	<u>20.60-10.18</u>	15	<u>+9.09-9.09</u>	
Tree	<u>9.00-3.11</u>	<u>44-43</u>	<u>-1.55-1.65</u>	<u>28.82-12.43</u>	28	<u>-8.52-8.81</u>	<u>42.74-22.14</u>	22	<u>-17.90-18.18</u>	

Table 4. Statistical scores for direct solar radiation received by surfaces before multiple reflections for summertime.

Config Units	Road			Walls			Tree		
	RMSE-MAE W m ⁻²	Err-MAPE %	Bias W m ⁻²	RMSE-MAE W m ⁻²	Err-MAPE %	Bias W m ⁻²	RMSE-MAE W m ⁻²	Err-MAPE %	Bias W m ⁻²
NVEG	8.91 <u>4.39</u>	1	-0.28	4.54 <u>2.49</u>	1	+0.40	-	-	-
A	18.32 <u>9.18</u>	14	+8.55 <u>-8.64</u>	6.86 <u>-3.52</u>	5	-1.55	10.04 <u>6.22</u>	4	-5.43
B1	22.78 <u>10.90</u>	9	+8.93 <u>-9.02</u>	21.12 <u>10.84</u>	6	+2.12	41.38 <u>19.22</u>	32	-13.17
B2	45.16 <u>22.86</u>	26	+22.06 <u>-22.28</u>	15.10 <u>8.26</u>	8	+2.25	47.44 <u>27.71</u>	37	-26.76
B3	31.23 <u>16.60</u>	22	+16.14 <u>-16.30</u>	21.80 <u>11.25</u>	20	+10.14	62.28 <u>37.07</u>	30	-36.78
B4	40.54 <u>20.59</u>	29	+20.01 <u>-20.22</u>	12.02 <u>-7.09</u>	8	-0.94	32.30 <u>19.44</u>	17	-18.35
C1	18.06 <u>9.01</u>	14	+8.38 <u>-8.46</u>	6.86 <u>-3.51</u>	5	-1.57	9.66 <u>5.96</u>	4	-5.18
C2	25.90 <u>13.67</u>	21	+13.20 <u>-13.33</u>	10.83 <u>-5.89</u>	9	-4.98	7.49 <u>4.13</u>	3	-3.17
C3	16.08 <u>8.31</u>	9	+7.64 <u>-7.72</u>	18.31 <u>9.77</u>	16	+8.67	43.87 <u>25.58</u>	22	-25.24
C4	21.82 <u>11.46</u>	13	+10.93 <u>-11.04</u>	9.22 <u>-4.77</u>	4	+1.58	25.15 <u>14.13</u>	18	-13.91
D1	23.23 <u>11.27</u>	6	+6.28 <u>-6.34</u>	18.74 <u>10.03</u>	5	+1.29	31.39 <u>14.95</u>	29	-8.86
D2	31.24 <u>15.69</u>	17	+14.98 <u>-15.14</u>	15.09 <u>8.29</u>	8	+2.23	35.87 <u>20.52</u>	30	-19.56
D3	12.91 <u>6.11</u>	4	+3.82 <u>-3.86</u>	14.45 <u>-7.82</u>	4	-1.68	29.52 <u>15.14</u>	20	-0.21
D4	38.66 <u>19.18</u>	21	+18.24 <u>-18.43</u>	9.32 <u>-5.05</u>	5	-3.57	25.90 <u>14.10</u>	23	-11.11

Table 5. Statistical scores for diffuse solar radiation received by surfaces before [multiple](#) reflections for summertime.

Config Units	Road			Walls			Tree		
	RMSE-MAE W m ⁻²	Err-MAPE %	Bias W m ⁻²	RMSE-MAE W m ⁻²	Err-MAPE %	Bias W m ⁻²	RMSE-MAE W m ⁻²	Err-MAPE %	Bias W m ⁻²
NVEG	<u>5.11-3.35</u>	7	+0.87	<u>2.59-1.70</u>	5	-0.43	-	-	-
A	<u>2.92-1.89</u>	15	<u>+1.34-1.36</u>	<u>2.72-1.51</u>	9	+1.07	<u>5.42-3.51</u>	20	-3.50
B1	<u>4.58-2.96</u>	14	<u>+1.87-1.89</u>	<u>3.16-1.83</u>	8	+1.09	<u>6.35-4.10</u>	43	-4.10
B2	<u>6.08-3.99</u>	29	<u>+3.72-3.75</u>	<u>2.81-1.64</u>	7	+0.79	<u>8.16-5.38</u>	49	-5.38
B3	<u>4.69-3.07</u>	24	<u>+2.69-2.72</u>	<u>4.83-2.88</u>	27	+2.72	<u>12.21-8.22</u>	44	-8.22
B4	<u>5.05-3.34</u>	30	<u>+3.15-3.18</u>	<u>2.51-1.47</u>	6	<u>-0.74+0.74</u>	<u>7.05-4.71</u>	32	-4.71
C1	<u>2.89-1.87</u>	14	<u>+1.29-1.30</u>	<u>2.53-1.50</u>	11	-0.55	<u>3.59-1.73</u>	13	<u>+0.24-0.24</u>
C2	<u>2.91-1.88</u>	14	<u>+1.33-1.34</u>	<u>2.48-1.60</u>	4	-0.19	<u>3.32-1.94</u>	12	-0.88
C3	<u>3.73-2.40</u>	13	<u>+1.49-1.51</u>	<u>3.02-1.69</u>	12	+1.38	<u>6.36-4.36</u>	28	-4.36
C4	<u>3.63-2.35</u>	13	<u>+1.47-1.49</u>	<u>2.69-1.69</u>	5	+0.52	<u>4.27-2.61</u>	22	-2.47
D1	<u>4.35-2.79</u>	10	<u>+1.28-1.30</u>	<u>2.54-1.53</u>	3	+0.36	<u>3.28-2.05</u>	26	-2.05
D2	<u>5.00-3.23</u>	20	<u>+2.68-2.71</u>	<u>2.29-1.40</u>	5	+0.25	<u>4.83-3.25</u>	35	-3.25
D3	<u>4.23-2.78</u>	9	<u>+1.08-1.09</u>	<u>2.55-1.63</u>	3	-0.11	<u>2.13-1.20</u>	17	-0.86
D4	<u>5.42-3.50</u>	22	<u>+3.01-3.04</u>	<u>2.48-1.62</u>	5	-0.65	<u>3.10-1.84</u>	27	-1.72

Table 6. Statistical scores for total (direct and diffuse) solar shortwave radiation absorbed by surfaces after multiple reflections for summer-time.

Config	Road			Walls			Tree		
	RMSE-MAE Units W m ⁻²	Err-MAPE %	Bias W m ⁻²	RMSE-MAE W m ⁻²	Err-MAPE %	Bias W m ⁻²	RMSE-MAE W m ⁻²	Err-MAPE %	Bias W m ⁻²
NVEG	9.88-6.03	3	+3.50	5.72-3.38	3	+2.80	-	-	-
A	19.67-13.32	27	+12.88-13.01	20.15-10.55	19-20	+10.18-10.44	14.53-8.85	5	-4.80-5.62
B1	21.00-13.24	14	+11.76-11.88	22.16-12.29	16	+11.85-11.89	41.70-21.69	29-30	-18.38-18.4
B2	39.02-24.11	32	+23.39-23.64	21.43-10.97	12	+10.26-10.30	52.64-31.72	41	-30.90-31.0
B3	33.61-21.74	36	+21.34-21.56	38.51-22.26	47	+22.10-22.26	86.57-54.26	38	-52.53-53.0
B4	36.65-23.03	39	+22.50-22.74	20.28-10.37	14	+8.87-9.04	35.32-22.03	19	-19.48-19.9
C1	18.18-12.18	23	+11.82-11.95	13.59-6.83	11	+5.49-5.73	16.71-9.46	8	-3.50-4.2
C2	24.27-16.08	31	+15.61-15.78	5.86-3.57	5	-0.26+0.06	13.99-7.53	4-3	+1.79-0.8
C3	19.71-13.31	20	+12.96-13.10	30.31-17.52	32	+17.37-17.52	68.13-43.16	31-32	-40.47-40.9
C4	23.59-15.88	23	+15.44-15.61	18.87-10.21	13-14	+10.02-10.21	41.20-24.38	24-25	-21.58-22.1
D1	20.13-12.41	11	+9.23-9.32	16.77-8.69	9	+7.59-7.63	30.17-15.74	27	-10.39-10.4
D2	27.11-17.15	21	+16.49-16.66	17.58-8.73	9	+7.54-7.58	37.21-22.15	29	-20.31-20.4
D3	13.87-9.02	9	+7.15-7.22	10.72-5.73	5	+4.53-4.58	24.50-13.27	8	-1.04-1.1
D4	32.65-19.91	25	+19.19-19.38	8.27-4.58	4	+2.61-2.65	23.95-13.54	23	-11.10-11.2